Chapter 12
Carbon Capture and Storage

12.1 Background Information

It has been accepted globally that carbon dioxide and several other gases known as greenhouse gases (GHGs) are causing global climate change by changing the physical and chemical processes in the Earth's upper troposphere and stratosphere. An independent record of the global average surface temperature shows that global warming is a fact of the past 130 years [5]. Although existing data published by different researchers differ from each other as a result of their data selection, processing, and bias corrections, they are leading to the same conclusion that global surface temperature has increased by 0.6–0.7 °C over the past century.

GHGs allow solar energy to enter the atmosphere freely. When sunlight strikes the surface of the Earth, some of the solar energy returns to space by reflection of infrared radiation. GHGs also absorb this infrared radiation and trap the heat in the atmosphere. If the amount of heat (or solar energy) from the Sun to the Earth's surface is the same as that leaving the Earth's surface to space, then the temperature of the Earth's surface remains stable. This perfect balance allows life to sustain on planet Earth.

However, there is an uncertainty in how the climate system varies naturally and reacts to extra GHGs. Making progress in reducing uncertainties in projections of future climate will require an understanding of the buildup of GHGs in the atmosphere and the behavior of the climate system.

The most important GHGs include carbon dioxide (CO_2), methane (CH_4), and nitrous oxide (N_2O). However, the most abundant greenhouse gas in the atmosphere is actually water vapor, which doubles the greenhouse effects caused by all the other GHGs. Some of the GHGs exist in nature and they include water vapor, carbon dioxide, methane, and nitrous oxide; others are exclusively human-made such as fluorinated gases are created solely by human activities. This is referred to as the "enhanced greenhouse effect" or the "anthropogenic greenhouse effect" as it is primarily due to the human activities.

Z. Tan, *Air Pollution and Greenhouse Gases*, Green Energy and Technology,
DOI 10.1007/978-981-287-212-8_12

Table 12.1 gives six leading GHGs that are under discussion in international climate change negotiations: CO_2, N_2O, CH_4, hydrofluorocarbons (HFC), perfluorocarbons (PFC), and sulfur hexafluoride (SF_6). All the GHGs do not contribute equally to the global climate change, therefore, global warming potential (GWP) is used to quantify the contribution to global warming for a unit mass of greenhouse gas, taking carbon dioxide as a reference with GWP = 1. More detailed information such as the calculation of GWP and lifetime of GHGs can be found in the IPCC [32] Report. The GWPs of other GHGs are higher than CO_2, due to difference in lifetime and radiation absorption behavior in the atmosphere. For example, the GWP of SF_6 is 23,900 times that of CO_2 due to its great stability and persistence. Its lifetime in atmosphere is estimated to be 3,200 years, making it the strongest GHG known today.

However, over all CO_2 is responsible for most of the greenhouse effect, only second to water vapor, due to its large total quantity. SF_6 contributes to approximately 0.1 % of the enhanced greenhouse effect.

CH_4 emissions mainly result from landfills, agriculture, coal mining, oil, and gas handling and processing. One of the solutions to this problem is to capture the CH_4 emission in a controlled environment, e.g., an anaerobic digester, and burn it into CO_2 to reduce its greenhouse effect. The chemical reaction is described as

$$CH_4 + 2O_2 \rightarrow CO_2 + 2H_2O \tag{12.1}$$

This reaction shows that one mole of CH_4 produces the same mole amount of CO_2. It, however, reduces the greenhouse effect by 20 times. And this is also the motivation behind flaring in the oil and gas industry.

N_2O emissions result from agriculture, chemical plants such as nitric acid or nylon processing units, and combustion processes. Fluidized bed combustion (FBC) is the most problematic with respect to N_2O emissions. Coal-fired FBC emits 50–150 times higher N_2O than pulverized coal firing plants. Vehicles emit more N_2O than stationary sources; a typical passenger car emits 20 mg/km N_2O in addition to 50 mg/km CH_4.

HFCs and PFCs are synthetic chemicals, produced as alternatives for the ozone-depleting chlorofluorocarbons (CFCs) in response to the "phase out" of CFCs under the Montreal protocol of 1987. HFC-134a is the major substitute for CFCs in refrigerators.

Table 12.1 Six leading GHGs and their GWPs (excluding water vapor)

GHG name	Formula	GWP
Carbon dioxide	CO_2	1
Methane	CH_4	21
Nitrous oxide	N_2O	310
Hydrofluorocarbons	HFC	140–11,700
Perfluorocarbons	PFC	7,400
Sulfur hexafluoride	SF_6	23,900

Source EIA [21]

Levels of GHGs have increased dramatically since the industrial revolution. For example, about 75 % man-made carbon dioxide emissions were from burning fossil fuels during the past 20 years. About 3.2 billion metric tons is added to the atmosphere annually. The U.S. produces about 25 % of global CO_2 emissions where 85 % of the US energy is produced through fossil fuel combustion [32]. Global carbon dioxide emissions continue increasing annually between 2001 and 2025, and the emerging economies (China and India, for example) contribute to much of the enhanced GHG effect. These developing countries' GHG emissions are expected to grow at 2.7 % annually by 2025 [22].

Combustion is the major source for the increase of CO_2 in the atmosphere. It can be concluded that reduction of CO_2 emissions from fossil fuel combustion will have the largest impact on GHG emissions. In this chapter, we focus primarily on approaches to CO_2 emission control. Readers are referred to the literature for the approaches to the GHG emission control.

12.2 CO_2 Generation in Combustion

According to IPCC [30–32] data, CO_2 emissions from large fossil fueled power plants account for half of the total carbon emissions. Other sources include industrial processes such as cement production, integrated steel mills, and oil-gas refinery. The mechanisms of CO_2 generation in combustion processes have been introduced in Parts I and II, and it is briefly summarized as follows for readers who are interested in this chapter only.

Stoichiometric combustion process of a hydrocarbon fuel $C_\alpha H_\beta$ perfectly mixed with oxygen can be described as

$$C_\alpha H_\beta + \left(\alpha + \frac{\beta}{4}\right) O_2 \rightarrow \alpha CO_2 + \frac{\beta}{2} H_2O \tag{12.2}$$

Thus the stoichiometry of a general hydrocarbon $C_\alpha H_\beta$ mixed with dry air perfectly can be described by the following formulas:

$$C_\alpha H_\beta + \frac{1}{\phi}\left(\alpha + \frac{\beta}{4}\right)(O_2 + 3.76N_2) \rightarrow \alpha CO_2 + \frac{\beta}{2} H_2O + \frac{3.76}{\phi}\left(\alpha + \frac{\beta}{4}\right) N_2 \tag{12.3}$$

where ϕ is the equivalence ratio.

The fuel-lean reaction formula for the combustion of $C_\alpha H_\beta$ perfectly mixed with excess air is

$$\begin{aligned} &C_\alpha H_\beta + \frac{1}{\phi}\left(\alpha + \frac{\beta}{4}\right)(O_2 + 3.76N_2) \\ &\rightarrow \alpha CO_2 + \frac{\beta}{2} H_2O + \frac{3.76}{\phi}\left(\alpha + \frac{\beta}{4}\right) N_2 + \left(\frac{1}{\phi} - 1\right)\left(\alpha + \frac{\beta}{4}\right) O_2 \end{aligned} \tag{12.4}$$

As introduced in combustion chemistry above, it is very challenging in engineering practices to achieve perfect mixing in the entire combustion device. Stoichiometric, fuel lean, and fuel rich combustion take place at different spots in the combustion device. As a result, the actual combustion formula is very complicated. One example formula is

$$\begin{aligned} &C_\alpha H_\beta + \frac{1}{\phi}\left(\alpha + \frac{\beta}{4}\right)(O_2 + 3.76\ N_2) \\ &\rightarrow [xCO_2 + (1-x)CO] + [yH_2O + (1-y)H_2] + \frac{3.76}{\phi}\left(\alpha + \frac{\beta}{4}\right)N_2 \\ &\quad + \left[\frac{1}{\phi}\left(\alpha + \frac{\beta}{4}\right) - \frac{1+x+y}{2}\right]O_2 \end{aligned} \tag{12.5}$$

where x and y in Eq. (12.5) can be determined by considering the chemical equilibrium reactions. The general chemical equilibrium formula for the reaction $aA + bB \leftrightarrow cC + dD$ is described in Eq. (12.6)

$$K_p = \frac{n_C^c n_D^d}{n_A^a n_B^b}\left(\frac{P}{n}\right)^{\Delta n} \tag{12.6}$$

where $\Delta n = c - d - a - b$. The chemical equilibrium constants based on partial pressure for chemical reactions with CO_2 and CO, $\ln(K_P)$, can be found in Table 12.2.

With the products described in Eq. (12.5), we can consider chemical equilibrium reactions to solve the unknowns of x and y.

Example 12.1: CO_2 emission rate calculation

Natural gas is fed into a burner at a rate of 1,000 m^3/h at 1 atm and 25 °C. Assuming that the air is premixed with $\phi = 1$, and the final products at equilibrium under 1,000 K and 1 atm contain O_2, N_2, CO_2, CO, H_2O, and H_2, determine the emission rate of CO_2 generation.

Solution

Assuming the natural gas is pure methane, with $\phi = 1$, $\alpha = 1$ and $\beta = 4$ Eq. (12.5) becomes

$$\begin{aligned} &CH_4 + 2(O_2 + 3.76N_2) \\ &\rightarrow [xCO_2 + (1-x)CO] + [yH_2O + (1-y)H_2] + 7.52N_2 + \left(\frac{3+x+y}{2}\right)O_2 \end{aligned}$$

Table 12.2 Equilibrium constants based on partial pressure for chemical reactions with CO_2 and CO

T (K)	$\ln(K_p)$	
	$CO_2 + H_2 \leftrightarrow CO + H_2O$	$CO_2 \leftrightarrow CO + {}^1/_2O_2$
298	−11.554	−103.762
500	−4.9252	−57.616
1,000	−0.366	−23.529
1,200	0.3108	−17.871
1,400	0.767	−13.842
1,600	1.091	−10.83
1,800	1.328	−8.497
2,000	1.51	−6.635
2,200	1.648	−5.12
2,400	1.759	−3.86
2,600	1.847	−2.801
2,800	1.918	−1.894
3,000	1.976	−1.111
3,200	2.022	−0.429
3,400	2.061	0.169
3,600		0.701
3,800		1.176
4,000		1.599

For each mole of CH_4, the total mole amount of products is

$$n = 11.02 + \frac{x+y}{2}$$

Consider two equilibrium reactions as follows:

$$CO_2 + H_2 \leftrightarrow CO + H_2O \quad (1)$$

$$CO_2 \leftrightarrow CO + {}^1/_2O_2 \quad (2)$$

The chemical equilibrium constants at 1,000 K can be found in Table 12.2.

$$K_{P1} = e^{-0.366} = 0.6935 = \frac{(1-x)y}{x(1-y)}$$

$$K_{P2} = e^{-23.529} = 6.046 \times 10^{-11} = \frac{1-x}{x}\frac{\left(\frac{3+x+y}{2}\right)^{1/2}}{\left(11.02+\frac{x+y}{2}\right)^{1/2}}$$

Reorganizing the equations leads to

$$\begin{cases} x = \dfrac{1}{1 + 0.6935\left(\frac{1-y}{y}\right)} \\ \dfrac{1-x}{x}\sqrt{\dfrac{3+x+y}{22.04+x+y}} = 6.046 \times 10^{-11} \end{cases}$$

Solving these equations with the assistance of software we can get

$$x \approx y \approx 1; 1 - x = 1.32 \times 10^{-10}; 1 - y = 1.91 \times 10^{-10}$$

The extremely low CO and H_2 concentration is a result of stoichiometric combustion at high temperature. Anyway, for each mole of CH_4, there is about 1 mol of CO_2 produced. At 1 atm and 25 °C, one mole of gas corresponds to 0.248 m^3/mol. Thus, the CH_4 feeding rate is 4032.26 mol/h. As a result, the CO_2 production rate is the same as 4032.26 mol/h, or

$$\dot{m}_{CO_2} = 44\frac{\text{kg}}{\text{kmol}} \times 4.032\frac{\text{kmole}}{\text{h}} = 177.42\,\text{kg/h}$$

12.3 General Approaches to Reducing GHG Emissions

Enhanced global warming effects can be reduced by reducing the emission of CO_2 and other GHGs. Emission reductions of CO_2 can be accomplished by a combination of several of the following approaches:

- Improved energy conversion efficiency in stationary and mobile combustion processes.
- Supply and end-use efficiency improvement and conservation.
- Shift to alternative energy sources, which have been introduced in Chap. 8. They are effective in air pollution control as well as carbon emission reduction.
- Carbon capture and storage (CCS).

Carbon emissions of CO_2 are inevitable as long as hydrocarbon fuels are used for energy conversion. However, more efficient combustion processes may produce less CO_2 per unit power generated. The CO_2 emissions per kWh power generated from a low efficiency coal-fired boiler may be 4 times that from a natural gas-fired gas turbine combined cycle plant (NGCC).

End-use efficiency improvements and energy conservation are the simplest and most cost-effective approaches to reduce carbon emissions and other air pollutants. For example, in the residential and commercial sectors, it can be achieved by reducing heating and air conditioning consumptions, better insulations, lowering hot water consumption, replacement of incandescent with fluorescent lighting, and

so on. It is estimated that in the residential-commercial sector in USA, by the year 2010, carbon emissions could be reduced by 10.5 % below 1990 levels with cost-effective conservation measures.

The follow sections focus on CCS.

12.4 Carbon Capture Processes

CCS refers to a number of technologies that capture CO_2 at some stage from processes such as combustion (most for power generation), gasification, cement manufacture, iron and steel making, and natural gas treatment. We introduce CCS in a generic way using combustion as main examples. Similar approaches can be taken for other industrial processes as well.

Like approaches to other air emission control, carbon capture can be achieved by pre-, in-, and post-combustion gas separation. The following topics are introduced in the section that follows.

- Pre-combustion carbon capture
  - Gasification and IGCC
- In-combustion carbon capture
  - Oxyfuel combustion
  - Chemical-looping combustion
- Post-combustion carbon capture
  - CO_2 capture from flue gas
  - CO_2 capture from atmosphere

12.4.1 Pre-combustion Carbon Capture

Pre-combustion carbon capture process is associated with the integrated gasification combined cycle (IGCC) [49]. Figure 12.1 shows the simplified process of IGCC with pre-combustion CO_2 capture. It is achieved by converting primary fossil fuels into hydrogen fuel. Hydrogen can be produced by partial oxidation of primary fuel for syngas followed by water shift and syngas purification, where CO_2 and other impurities are removed.

12.4.1.1 Syngas Production

Partial oxidation of a primary fuel is a highly fuel rich combustion process as described in Eq. (12.5). Since the process aims at the conversion of solid fuels into gaseous

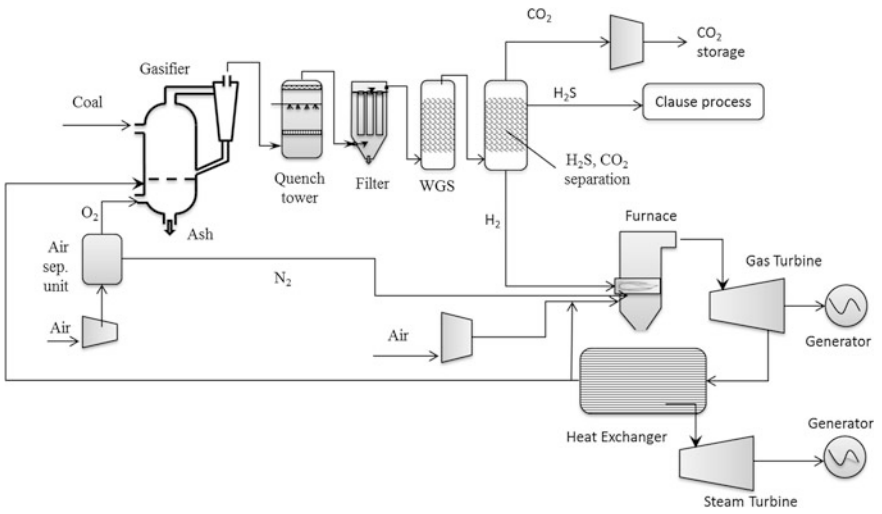

Fig. 12.1 Simplified IGCC with pre-combustion CO_2 capture process

products, it is commonly called gasification. Unlike a conventional combustion process where we expected as little CO and H_2 as possible, the gasification process aims to maximize the production of CO and H_2, which are the main compounds of syngas. Since the partial oxidation temperature is much lower than that required for thermal NO_x formation, the produced syngas is mainly a mixture of CO and H_2 with other trace amounts of impurities such as NH_4, H_2S, SO_2, and particulates.

Advanced gasification process employs oxygen as an oxidant in order to reduce nitrogen-introduced impurities, and the overall reaction can be described as

$$C_\alpha H_\beta + \frac{1}{\phi}\left(\alpha + \frac{\beta}{4}\right)O_2 \rightarrow [xCO_2 + (1-x)CO] + [yH_2O + (1-y)H_2] + zO_2 \tag{12.7}$$

Oxygen is usually produced by separation of nitrogen from the air in an air separation unit (see Fig. 12.1). In return, the formation of thermal NO_x is minimized.

One way or another, an ideal partial oxidation process should aim at $x, y \rightarrow 0$.

In practice, solid fuels (e.g., coal and biomass) and methane are used for partial oxidation. When solid fuels are used, the corresponding simplified chemical reactions are described as follows:

$$C(s) + \frac{1}{2}O_2 \rightarrow CO \qquad \text{Carbon partial oxidation} \tag{12.8}$$

$$C(s) + H_2O \rightarrow CO + H_2 \qquad \text{Carbon steam reaction} \tag{12.9}$$

$$C(s) + CO_2 \rightarrow 2CO \qquad \text{Boudouard reaction} \qquad (12.10)$$

Partial oxidation of methane can be described as

$$CH_4 + \frac{1}{2}O_2 \rightarrow CO + 2H_2 \qquad \text{Methane partial oxidation} \qquad (12.11)$$

$$CH_4 + H_2O \rightarrow CO + 3H_2 \qquad \text{Steam methane reaction} \qquad (12.12)$$

The steam-methane reaction is effective in the temperature range of 700–950 °C at 1.4–4 MPa. Under these conditions, 70–80 % of the methane can be converted into hydrogen in one single reactor.

The syngas can be directly burned for energy production where CO is converted into CO_2 by oxidation, but water–gas shift (WGS) is necessary to facilitate pre-combustion carbon capture. The CO produced in partial oxidation process eventually is converted into CO_2 by the WGS reaction

$$CO + H_2O \rightarrow H_2 + CO_2 \qquad (12.13)$$

Typical syngas composition after WGS is shown in Table 12.3. The high concentration of CO_2 favors effective CO_2 capture.

By the WGS reaction over 90 % of the carbon exist as CO_2. For the processes aiming at high purity H_2, CO_2 removal efficiency has to be improved. This is achieved commonly by multiple CO_2 removal units.

Table 12.3 Composition of typical gases subjected to pre-combustion and post-combustion CO_2 separation

Gases	Mole fraction	
	Pre-combustion syngas after WGS reaction	Post-combustion flue gas
CO_2	37.7 %	10–15 %
H_2O	0.14 %	5–10 %
H_2	55.5 %	
NO_x		<1,000 ppm
SO_x		<1,000 ppm
O_2		3–4 %
CO	1.7 %	20 ppm
N_2	3.9 %	70–75 %
H_2S	0.4 %	
Temperature	40 °C	40–75 °C
Pressure	30 atm	1 atm

Sources D'Alessandro et al. [17] and Ramdin et al. [49]

12.4.2 In-combustion Carbon Capture

12.4.2.1 Oxyfuel Combustion

In-combustion carbon capture is achieved primarily by oxyfuel combustion. Oxygen rather than air is used as oxidizer in combustion. Then the main combustion products, as described using Eq. (12.2), are CO_2 and water. Depending on the fuel composition, there may be SO_2, NO_x and others, but thermal NO_x is greatly reduced. As a result, the CO_2 can be readily separated from water and other trace compounds for transport and storage.

The oxyfuel combustion process is a promising concept but still under research and development (R&D). The fuels fed into an oxyfuel combustion system can be natural gas, biomass, or coal. A simplified schematic diagram of oxyfuel combustion with CO_2 capture process is shown in Fig. 12.2. Unlike conventional combustion technologies, this process utilizes oxygen instead of air as the oxidant, thereby eliminating nitrogen in the downstream separation. The corresponding simplified combustion stoichiometry is described using

$$C_\alpha H_\beta + \left(\alpha + \frac{\beta}{4}\right) O_2 \rightarrow \alpha CO_2 + \frac{\beta}{2} H_2O \tag{12.14}$$

Example 12.2: Oxyfuel computation flame temperature
In Sect. 3.5.1, we calculated the adiabatic flame temperature of CH_4 burned with air at 298 K, when they are premixed perfectly with an equivalence ratio of 1.0 and the combustion is complete. Now let us redo the calculation using pure oxygen instead of air. Determine the corresponding constant pressure adiabatic flame temperature.

Solution
First of all, set up stoichiometric combustion reaction equation, using the methods introduced in Sect. 3.4,

$$CH_4 + 2O_2 \rightarrow CO_2 + 2H_2O$$

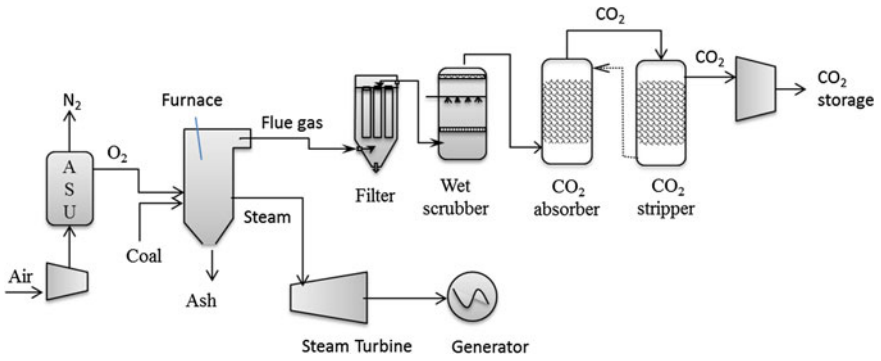

Fig. 12.2 Schematic diagram of the oxyfuel combustion process for CO_2 capture

For an adiabatic constant pressure system, with the reactant temperature of $T_R = T_0 = 298$ K, the left-hand side (LHS) of Eq. (12.15)

$$\sum_R n_i \left[\left(a_i (T_R - 298\,\mathrm{K}) + \frac{b_i}{2} (T_R^2 - (298\,\mathrm{K})^2 \right) + h_{f,i}^o \right] = \sum_P n_i \left[\left(a_i (T_a - 298\,\mathrm{K}) + \frac{b_i}{2} (T_a^2 - (298\,\mathrm{K})^2 \right) + h_{f,i}^o \right] \tag{12.15}$$

becomes

$$\mathrm{LHS} = h_{f,\mathrm{CH_4}}^o + 2h_{f,\mathrm{O_2}}^o \tag{1}$$

The right-hand side (RHS) of the equation is simplified as

$$\mathrm{RHS} = \left[\left(a_{\mathrm{CO_2}} (T_a - 298\,\mathrm{K}) + \frac{b_{\mathrm{CO_2}}}{2} (T_a^2 - (298\,\mathrm{K})^2 \right) + h_{f,\mathrm{CO_2}}^o \right] + 2 \left[\left(a_{\mathrm{H_2O}} (T_a - 298\,\mathrm{K}) + \frac{b_{\mathrm{H_2O}}}{2} (T_a^2 - (298\,\mathrm{K})^2 \right) + h_{f,\mathrm{H_2O}}^o \right] \tag{2}$$

Looking into Table A.4, we can get the parameters needed (Table 12.4)

Substituting these values into Eq. (1) and Eq. (2) leads to

$$\mathrm{LHS} = -74{,}980\,(\mathrm{J/mole})$$

$$\mathrm{RHS} = \left[\left(44.3191 (T_a - 298) + \frac{0.0073}{2} (T_a^2 - (298\,\mathrm{K})^2 \right) - 394{,}088 \right] + 2 \left[\left(32.4766 (T_a - 298\,\mathrm{K}) + \frac{0.00862}{2} (T_a^2 - (298\,\mathrm{K})^2 \right) - 242{,}174 \right]$$

Simplification of the equation gives

$$0.01227 T_a^2 + 109.2723\, T_a - 837109 = 0$$

Solving this equation we can get, $T_a = 4930.8$ K. This calculated value is much higher that air-fuel combustion: $T_a = 2341$ K.

Table 12.4 Parameters used in Example 1.22

Species	$h_{f,i}^o$ (J/mole)	$C_p(T)$ (J/mole · K)	
		a_i	b_i
CO_2	−394,088	44.3191	0.0073
H_2O	−242,174	32.4766	0.00862
O_2	0	30.5041	0.00349
CH_4	−74,980	44.2539	0.02273

Although it is only estimation, the comparison does show that the oxyfuel combustion flame temperature is higher than that of conventional combustion with air. As a result, the boiler of the oxyfuel combustion process requires special materials that can survive extreme temperature.

Another concern of the oxyfuel combustion process with sulfur containing fuels is the high SO_x concentration without the dilution of nitrogen, resulting in high corrosion on the ducts. Extra costs are associated with concentrated oxygen production by costly air separation units.

The benefit is a simple process for carbon capture after combustion. Without nitrogen and NO_x in the flue gas, it contains mainly H_2O and CO_2. After the removal of soot and SO_2, if any, CO_2 can be readily separated from water vapor by condensation in a cooler. This highly concentrated CO_2 is ready for transportation and storage.

12.4.2.2 Chemical Looping Combustion

Similar to oxyfuel combustion, chemical-looping combustion is an emerging combustion process that is attractive for the benefit of carbon capture. This idea was first introduced by Lewis and Gilliland [38] as a way to produce pure CO_2 from fossil fuels. Thirty years later, Ishida et al. [33] proposed the use of chemical-looping combustion for power generation with climate mitigation. Figure 12.3 shows an example schematic diagram of chemical-looping combustion based on circulating fluidized bed principle. Most of the state of the art focuses on gaseous fuels reacting with oxygen carrier. Similar principles can be applied to the oxidation of the vapors of liquid fuels and volatiles released from solid fuels.

The combustion in the fuel reactor takes place following different reaction steps. The oxygen-needed is released from the oxygen-carrier (Me_xO_y) at high temperature.

$$2Me_xO_y \leftrightarrow 2Me_xO_{y-1} + O_2 \tag{12.16}$$

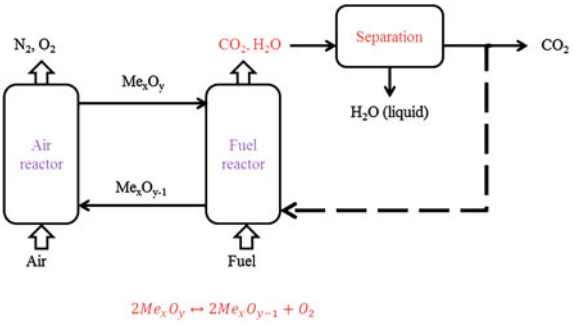

Fig. 12.3 Schematic diagram of the chemical looping combustion

The reduced oxygen-carrier Me_xO_{y-1} is regenerated in the air reactor according to the reverse reaction in Eq. (12.16), where the oxygen is from the air. Effluent gases from the air-reactor containing air with reduced amount of oxygen can be discharged without negative environmental impact, and the regenerated solid oxygen carrier is transported to the fuel reactor, and another cycle starts.

The key of this technology is the special oxygen carrier! About one thousand oxygen carrier materials have been studied in laboratory [2]. The first-generation oxygen carriers focused on mainly oxides of four metals: Ni, Fe, Mn, and Cu. Recent advances focused on low cost materials by combing different metal oxides and oxygen releasing materials aiming at solid fuel combustion. Among many combined materials tested in laboratory, very few have been tested in continuous operation. Most researchers have used ilmenite ($FeTiO_3$) [8, 15] because of its low cost and reasonably high reactivity towards syngas.

This process must enable the release of oxygen from the oxygen-carriers. Thereby, only those metal oxides that have a suitable equilibrium partial pressure of oxygen at temperatures of interest for combustion (800–1,200 °C) can be used as oxygen-carriers. These materials include, but are not limited to CuO/Cu_2O, Mn_2O_3/Mn_3O_4, and Co_3O_4/CoO [34]. Operating conditions in the air-reactor and fuel-reactor would be determined for specific oxygen-carrier [50].

Three example metal oxides are as follows:

$$4CuO \leftrightarrow 2Cu_2O + O_2 \tag{12.17}$$

$$6Mn_2O_3 \leftrightarrow 4Mn_3O_4 + O_2 \tag{12.18}$$

$$2Co_3O_4 \leftrightarrow 6CoO + O_2 \tag{12.19}$$

Then the oxygen reacts with the gas fuel or char and volatiles (mainly H_2, CO, CH_4) from the solid fuels following the combustion principles.

$$\text{Gases} + \text{Volatiles} + \text{Char} + O_2 \rightarrow CO_2 + H_2O \tag{12.20}$$

If we take CH_4, H_2 and CO as examples, the overall chemical reactions are

$$CH_4 + 2O_2 \rightarrow CO_2 + 2H_2O \tag{12.21}$$

$$H_2 + \frac{1}{2}O_2 \rightarrow H_2O \tag{12.22}$$

$$CO + \frac{1}{2}O_2 \rightarrow CO_2 \tag{12.23}$$

As described in Eq. (12.20), the ultimate goal of chemical-looping combustion is to convert fuel into carbon dioxide and water without NO_x. The degree of fuel

conversion to CO_2 and H_2O is quantified using the gas yield; which is defined as the fraction of the fuel oxidized to CO_2 or H_2O. Similar to the approaches in oxyfuel combustion, water vapor is removed from highly concentrated CO_2 stream that can be compressed for transport and storage.

12.4.3 Post-combustion Carbon Capture

Post-combustion CO_2 capture is mainly achieved by flue gas cleaning for stationary sources such as a power plant and an industrial facility. Unlike pre-combustion and oxyfuel combustion approaches, post-combustion carbon capture technologies are more complex due to more air powered combustion-related air contaminants. Capture of most of the contaminants has been introduced in the other chapters of this book.

CO_2 separation is enabled after all the post-combustion air cleaning processes introduced in the chapter for post-combustion air emission control. As shown in Table 12.3, the cleaned flue gas usually contains 10–15 % of CO_2 that is diluted by nitrogen gas. Therefore, an effective post-combustion CO_2 separation technology should be able to cope with low CO_2 partial pressure. In general, physical sorption is not effective for separation of gases with low partial pressure. Therefore, we should focus on chemisorption technologies for post-combustion CO_2 capture.

If we consider low CO_2 partial pressure as a disadvantage of post-combustion CO_2 capture, this disadvantage is compensated with its flexibility in retrofitting an existing facility without major modifications. Capture ambient CO_2 has been proposed as well. It can be considered as an alternative CO_2 capture process, but at temperatures lower than those of combustion flue gases before discharge.

Despite the differences in pre- and post-combustion approaches, CO_2 must be separated from the carrier gas. They share the fundamentals introduced in Chap. 5, primarily the separation of gas (CO_2 specifically) from the mixture. However, at the time of writing this book, all the CCS projects are under pilot tests. No single large-scale plant with CCS is known to be operational continuously.

The major barrier to the commercialization of CCS process at large scale is the high costs associated with carbon separation, transport, and injection. Currently, the most widely used technology for CO_2 separation is based on amine-solvents, for example, monoethanolamine (MEA). A large amount of energy is required for solvent regeneration. The energy consumption rate, assuming a 30 wt% MEA (aqueous) solution and 90 % of removal efficiency, was estimated to be in the range of 2.5–3.6 GJ per ton of CO_2. Additional energy consumption for compressing the captured CO_2 to the required pressure of 150 bar for transportation and storage is 0.42 GJ/ton CO_2. These numbers can be transferred to extra costs of $50–150 per ton CO_2 removed using amines [18]. The existing CCS technologies are far from being cost-effective and unattractive for large-scale applications. Much more research is needed for design of low-cost sorbents and optimized process design CO_2 capture. Our focus that follows is on the sorbent and related process design.

12.5 CO_2 Separation by Adsorption

CO_2 can be separated from a gas stream by both physical adsorption and chemical adsorption. The general differences between a physical and chemical adsorption has been introduced in Chap. 5. Physical CO_2 adsorption operates at temperatures lower than 100 °C; whereas the chemical counterpart operates at a high range of 400–600 °C.

12.5.1 Physical Adsorption

A good CO_2 physical adsorbent is expected to be characterized with high affinity with CO_2 compared to other gases in the stream, high adsorption capacity, low heat of adsorption, low adsorption hysteresis, and steep adsorption isotherm. These features ensure the cost-effectiveness of the operation with high efficiency, low energy consumption, and low material cost.

The best adsorbent is expected to be characterized with high CO_2 capacity at low pressure, high selectivity for CO_2, fast adsorption/desorption kinetics, good mechanical properties, high hydrothermal and chemical stability, as well as low costs of synthesis. Unfortunately, these criteria are too ideal for any single adsorbent.

The most widely investigated low temperature CO_2 adsorbents are zeolites and activated carbons. Compare to Zeolite-13X and natural zeolite, activated carbon showed higher carbon adsorption capacity and steepest isotherm, but high hysteresis challenges the desorption process.

Metal–organic frameworks (MOFs) have recently attracted intense research interest in CO_2 adsorption due to their large porous volume and surface areas [42, 43]. In general, the CO_2 adsorption in MOFs varied with CO_2 pressure. At high pressures, CO_2 adsorption capacities depend on surface areas and pore volumes of the MOFs. Otherwise, the capacities depend on the heat of adsorption. In addition, many MOFs have shown high CO_2/N_2 and CO_2/CH_4 selectivity. However, there are two important challenges to MOFs into practical applications of CO_2 capture:

(1) the mass production of MOFs at low cost
(2) the stabilities of MOFs toward moisture, other acid gases, and heat for regeneration.

Interested readers are encouraged to conduct a state-of-the-art literature review in this area of research.

Continuous CO_2 adsorption can be implemented by a pressure swing adsorption process. It is widely used for air drying using synthetic zeolites or activated alumina

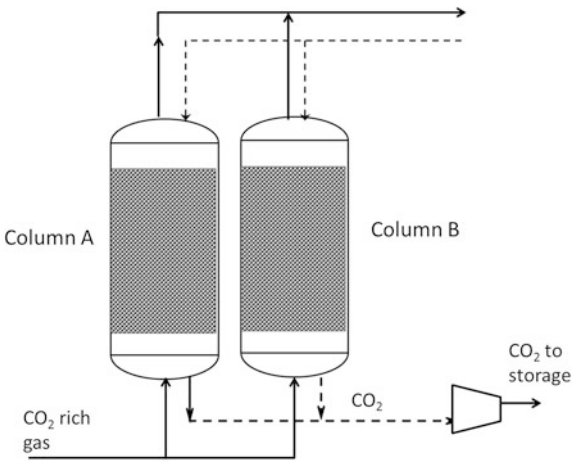

Fig. 12.4 Schematic diagram of pressure swing adsorption process

for moisture removal. Advances in pressured swing adsorption can be found in the state of the art provided by Grande [24]. A pressure swing adsorption (PSA) process has at least two columns, when one is working on CO_2 adsorption from the high pressure gas, the used sorbent in other column is regenerated at low pressure. A simple PSA process for CO_2 capture is shown in Fig. 12.4.

12.5.2 Chemical Adsorbents

Chemical adsorption at high temperature (400–600 °C) has a potential for pre-combustion CO_2 capture and hydrogen production. High temperature sorbent can be employed for carbon separation without temperature quenching and consequently do not comprise much with overall energy efficiency. The working principles are similar to those of calcium based adsorption.

12.5.2.1 Calcium-Based Adsorbent

CaO is one of the oldest sorbent for CO_2 capture by chemical adsorption. Calcium oxide reacts with CO_2 at high temperatures to produce carbonates:

$$CaO_{(s)} + CO_2 \leftrightarrow CaCO_{3(s)} \tag{12.24}$$

where (*s*) stands for solid state. The forward reaction takes place at about 600–800 °C, and the backward reaction at higher temperature (>870 °C) may result in sorbent regeneration by decarbonation and releasing CO_2.

Calcium-based sorbents are commonly produced from limestone. Sometimes, sorbents that are produced from calcined dolomite ($CaCO_3 \cdot MgCO_3$) or huntite ($CaCO_3 \cdot 3MgCO_3$) contain MgO. MgO does not react with CO_2 at 600–800 °C, but its presence helps with the lifetime and durability of the calcium-based sorbent. Since CaO degrades quickly after a few cycles of regeneration, more reliable sorbents have been developed and tested at high temperatures; they include Calcium aluminate ($CaAl_2O_4$), Sodium Zirconate (Na_2ZrO_3), Lithium zircanate (Li_2ZrO_3), and Lithium orthosilicate (Li_4SiO_4).

12.5.2.2 Temperature Swing Adsorption Process

By taking advantage of this reversible reaction (12.24) between CO_2 and CaO at different temperatures, a temperature swing adsorption-desorption system allows continuous chemical adsorption of CO_2. The schematic diagram for syngas cleaning by separating CO_2 from syngases is shown in Fig. 12.5. Similar process can be employed for the post-combustion carbon capture system. Alternatively, the sorbent can also be lithium silicate, which can be regenerated at a lower temperature of 800 °C.

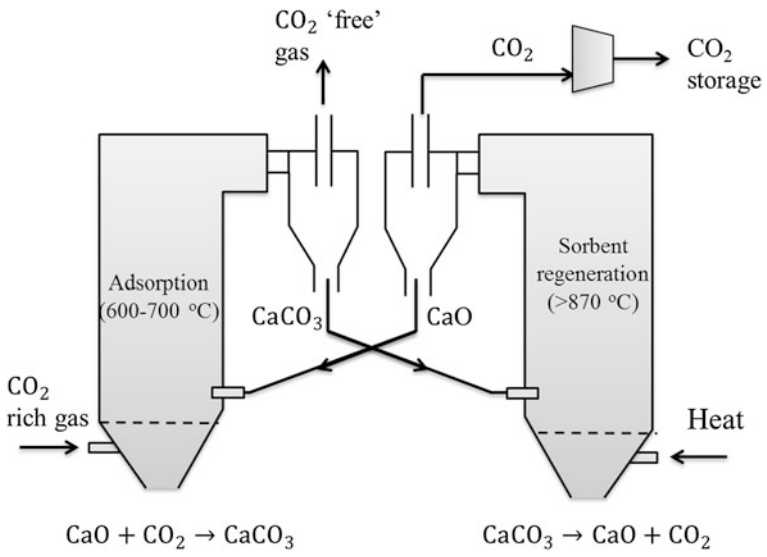

Fig. 12.5 Schematic diagram of temperature swing carbon capture process

12.6 CO_2 Separation by Absorption

CO_2 absorption can also be classified into physical and chemical absorptions. Physical absorption requires much lower energy to regenerate the solvent than chemical absorption. A conceptual comparison between chemical and physical absorption capacity at different absorbate partial pressures is shown in Fig. 12.6. Physical absorption is not economical for absorption of gases with a low partial pressure, say from the combustion flue gas. It aims at compressed gases.

12.6.1 Physical Absorption

Physical absorption processes use organic or inorganic solvents to absorb CO_2 from the carrier gases. The process capacity is governed by Henry's law described in Eq. (2.76); the equilibrium solubility of CO_2 in a solvent is

$$c_{CO_2} = \frac{P_{CO_2}}{H} \tag{12.25}$$

where c_{CO_2} is the equilibrium CO_2 concentration in the solvent, P_{CO_2} is the CO_2 partial pressure in the gas phase, and H is the corresponding Henry's constant. Practically speaking, solvent with a great CO_2 solubility is preferred at a reasonable cost for physical CO_2 absorption.

Physical absorption is primarily used for high pressure CO_2 separation to increase the solubility in the solvent. Refrigerated methanol (CH_3OH) was considered an effective CO_2 solvent for CO_2 sequestration at low temperature. The solubility of CO_2 in methanol at −10 °C and $P_{CO_2} = 1$ atm is 10 L of CO_2 per liter of methanol, which is 4 times that of water.

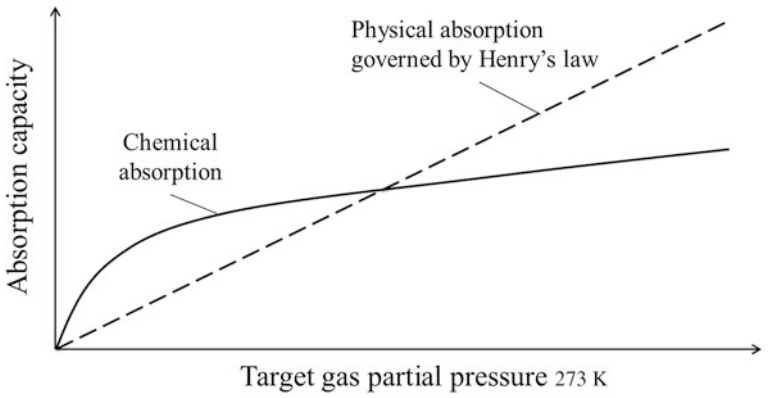

Fig. 12.6 Relative solvent loading versus partial pressure of the absorbate gas

12.6.2 Amine-Based Chemical Absorption

Chemical absorption is suitable for CO_2 capture at low pressure and low temperature. The sorbents used for chemical absorption include carbonate-based, sodium hydroxide-based, aqueous ammonia-based, and amine-based sorbents.

Amine-based CO_2 absorption is a relatively mature technology used in the ammonia process, steam reforming process, and the natural gas sweetening process. Amines are ammonia-derived organic compounds when one or more hydrogen atom(s) of ammonia are replaced with organic substituents. Amines are classified as primary, secondary, and tertiary amines based on the number of replaced hydrogen atoms.

The choice of amine for CO_2 absorption depends on three key factors: rate of reaction, regeneration energy, and loading capacity. The ideal solvent is characterized with a great rate of reaction, low regeneration energy, and great loading capacity. However, none of the alkanolamines meets all these three requirements. In general, the rate of reaction follows the order of *primary* > *secondary* > *tertiary*; the order is reversed for regeneration energy and loading capacity [35]. Ethanolamine (C_2H_7NO or 2R-NH_2), also called 2-*aminoethanol* or *monoethanolamine* (*MEA*) is the most commonly used amine for CO_2 absorption. It is a primary amine, and a alcohol too.

Among all the amines tested, MEA showed its high reactivity with CO_2, and is predominantly used for CO_2 capture in the industry. Aqueous amine solutions are bases and the pKa values of typical alkanolamines are listed in Table 12.5. Thereby, amines can react with not only CO_2 but also other acidic gases like SO_2 and NO_2 at great rates of reactions. Therefore, SO_2 and NO_2 have to be effectively removed first before CO_2 absorption if it is to be used for post-combustion carbon capture. It also reduces the contamination to the regenerated solvent and recovered CO_2.

12.6.2.1 Kinetics of Amine-CO_2 Reactions

As the most popular CO_2 absorbent, the kinetics of CO_2 reaction with alkanolamines deserves an in-depth discussion. The reaction of CO_2 with primary and secondary

Table 12.5 pKa values of base amines at 298 K

Amine		pKa
MEA	Monoethanolamine	9.50
DEA	Diethanolamine	8.88
DIPA	Diisopropanolamine	8.80
TEA	Triethanolamine	7.76
MDEA	Methyldiethanolamine	8.57
AMP	2-Amino-2-methyl propanol	9.70
DEMEA	Diethylmonoethanolamine	9.82

Source: [54]

amines is usually described by the *zwitterion mechanism*, whereas the reaction with tertiary amines is described by the base-catalyzed hydration of CO_2 [54].

According to the zwitterion mechanism [16] the reaction between CO_2 and the amine (AmH) proceeds through the formation of a zwitterion as an intermediate (R1, Eq. (12.27)).

$$CO_2 + AmH \underset{k_{b1}}{\overset{k_{f1}}{\leftrightarrow}} AmH^+COO^- \qquad (R1) \qquad (12.27)$$

The zwitterion reacts with a base or bases (Bs) to form carbamate as the final product (R2, Eq. (12.28)).

$$AmH^+\ COO^- + Bs \overset{k_B}{\rightarrow} AmCOO^- + BsH^+ \qquad (R2) \qquad (12.28)$$

When the base is MEA its self, Eqs. (12.27) and (12.28) lead to an overall reaction. It shows that the stoichiometric CO_2 to MEA mole ratio is 0.5 mol CO_2 per mole of MEA.

With water in the solution, the following reactions may also take place:.

$$H_2O \leftrightarrow H^+ + OH^- \qquad (12.29)$$

$$CO_2 + OH^- \overset{k_{OH}}{\leftrightarrow} HCO_3^- \qquad (R3) \qquad (12.30)$$

$$CO_2 + H_2O \overset{k_{H_2O}}{\leftrightarrow} HCO_3^- + H^+ \qquad (R4) \qquad (12.31)$$

Assuming zwitterion concentration at quasi-steady state, the overall rate of reaction for R1 and R2 is

$$r_{1,2} = k_{f1}[CO_2][AmH] - k_{b1}[AmH^+COO^-] = k_B[AmH^+\ COO^-][Bs] \qquad (12.32)$$

Reorganizing Eq. (12.32) leads to

$$\frac{r_{1,2}}{[CO_2][AmH]} = \frac{k_{f1}}{1 + k_{b1}/(k_B[Bs])} \qquad (12.33)$$

When R2 is instantaneous, $k_{b1} \ll k_B$, as it is for some amines. Almost every zwitterion is deprotonated before it can revert to CO_2 and amine through the backward reaction in R1. Mathematically, the denominator in Eq. (12.33) can be simplified by $k_{b1}/(k_B[Bs]) \rightarrow 0$ and Eq. (12.33) becomes

$$r_{1,2} = k_{f1}[CO_2][AmH] \qquad (12.34)$$

The rate of reaction for R3 and R4 are, respectively,

$$r_3 = k_{OH}[CO_2][OH^-] \tag{12.35}$$

$$r_4 = k_{H_2O}[CO_2][H_2O] \tag{12.36}$$

Combination of Eqs. (12.33), (12.35) and (12.36) leads to the overall CO_2 reaction rate by summation of $r_{1,2}$, r_3 and r_4:

$$r_{CO_2} = \left\{ \frac{k_{f1}[AmH]}{1 + k_{b1}/(k_B[Bs])} + k_{OH}[OH^-] + k_{H_2O}[H_2O] \right\}[CO_2] \tag{12.37}$$

Denote the part in the { } bracket as *observed reaction rate* with respect to CO_2, k_{CO_2}:

$$k_{CO_2} = \frac{k_{f1}[AmH]}{1 + k_{b1}/(k_B[Bs])} + k_{OH}[OH^-] + k_{H_2O}[H_2O] \tag{12.38}$$

where the first term is called *apparent reaction rate constant*

$$k_{app} = \frac{k_{f1}[AmH]}{1 + k_{b1}/(k_B[Bs])} \tag{12.39}$$

Similar to the denotation of $k_{OH}[OH^-] + k_{H_2O}[H_2\ O]$, we can define the reaction rate constant with respect to amine as

$$k_{AmH} = \frac{k_{f1}}{1 + k_{b1}/(k_B[Bs])} \tag{12.40}$$

Then Eq. (12.38) becomes,

$$k_{CO_2} = k_{AmH}[AmH] + k_{OH}[OH^-] + k_{H_2O}[H_2O] \tag{12.41}$$

And Eq. (12.37) becomes

$$r_{CO_2} = k_{CO_2}[CO_2] \tag{12.42}$$

Many researchers have reported k_{AmH} for different amines at different conditions and some are listed in Table 12.6.

12.6.2.2 CO_2 Absorption Rate

The actual rate of CO_2 absorption into amine is an important indicator of energy consumption of the solvent. A fast rate of CO_2 absorption minimizes energy use in

Table 12.6 k_{AmH} for different amines

Amine	Reaction rate constant (m^3/kmole · s)	T (K)	Conc. (kmole/m^3)	References
AEEA	$k_{AEEA} = 6.07 \times 10^7 \exp\left(-\frac{3030}{T}\right)$	305–322	1.19–3.46	[44]
DEMEA	$k_{DEMEA} = 9.95 \times 10^7 \exp\left(-\frac{6238}{T}\right)$	298–313		[40]
MDEA	$k_{MDEA} = 4.61 \times 10^8 \exp\left(-\frac{5400}{T}\right)$	303–313		[36]
MEA	$k_{MEA} = 4.61 \times 10^9 \exp\left(-\frac{4412}{T}\right)$	293–333	3–9	[1]
EMEA	8,000	298	0.028–0.082	[40]
AEPD	378	303	5–25 wt%	[57]
AMP	810.4	298	0.25–3.5	[56]
DEA	2,375	298	0.25–3.5	[56]
DIPA	2,585	298	0.25–3.5	[56]

an optimized system. As explained in Chaps. 2 and 5, it depends on the rate of mass transfer from gas to liquid phases. CO_2 is typically absorbed by the process of diffusion with fast reactions in the liquid films. An optimized absorber design requires 90 % CO_2 removal with a reasonable amount of packing materials in the scrubber.

According to the double film theory introduced in Sect. 2.3.4, the overall gas side mass transfer coefficient (K_G) is related to the gas film mass transfer coefficient k_g and the liquid film mass transfer coefficient k'_g as

$$\frac{1}{K_G} = \frac{1}{k'_g} + \frac{1}{k_g} \tag{12.43}$$

Then the CO_2 flux by absorption can be described as

$$CO_2 \text{ Flux} = K_G\left(P_{CO_{2,g}} - P^*_{CO_2}\right)_{LM} = k'_g\left(P_{CO_{2,\text{interface}}} - P^*_{CO_{2,\text{bulksolution}}}\right) \tag{12.44}$$

Assume that the concentration of free amine in the liquid film is the same as the bulk liquid, the liquid film mass transfer coefficient, k'_g, can be estimated using [9, 41].

$$k'_g \approx \frac{(k_{AmH} D_{CO_2}[AmH])^{\frac{1}{2}}}{H_{CO_2}} \tag{12.45}$$

where k'_g has a unit of $mol/(m^2 \cdot Pa)$; it is sometimes also referred to as the normalized absorption flux of CO_2. D_{CO_2} is the diffusivity of CO_2 in the liquid (amine), k_{AmH} is the reaction rate constant of CO_2, [AmH] is the free amine concentration in the bulk solution, and H_{CO_2} is the Henry's law constant of CO_2 over the solvent.

Table 12.7 k'_g for different amines [9]

Amine	$k'_g \times 10^7$ mole/(m^2 · Pa)	Capacity (mole/kg)
Piperazine (PZ)	8.5	0.79
PZ/bis-aminoethylether	7.3	0.67
2-Methyl PZ/PZ	7.1	0.84
2-Methyl PZ	5.9	0.93
2-Amino-2-methyl propanol (AMP)	2.4	0.96
PZ/aminoethyl PZ	8.1	0.67
PZ/AMP	7.5	0.70
Hydroxyethyl PZ	5.3	0.68
PZ/AMP	8.6	0.78
2-Piperidine ethanol	3.5	1.23
Monoethanolamine (MEA)	3.6	0.66
MEA	4.3	0.47
Methydiethanolamine (MDEA)/PZ)	8.3	0.99
MDEA/PZ	6.9	0.80
Kglycinate	3.2	0.35
Ksarconinate	5	0.35
MEA/PZ	7.2	0.62

The measured k'_g for different amines and amine alternatives are summarized in Table 12.7. There is no obvious correlation between the mass transfer coefficients and the capacities of different amines.

12.6.2.3 Amine-Based CO_2 Capture Process

MEA is considered the baseline solvent for CO_2 capture. The design of a MEA based CO_2 absorption tower follows the principles introduced in Sect. 5.2. In a typical CO_2 scrubber, the flue gas at 40–60 °C enters the tower from the bottom while a 20–30 wt% MEA solution flows downward continuously from the top. Because MEA is corrosive, diluted instead of concentrated MEA is used. After selective absorption of CO_2 from the flue gas, the CO_2-rich amine solution is drained off from the bottom of the absorber.

The rich solvent is regenerated in a stripper that operates at 100–140 °C. The energy required for solvent regeneration can be from waste heat recovery from a steam and/or a reboiler. A high-efficiency heat exchanger can also be employed to recycle the heat from the rich solvent from the absorber tower. The recovered gas phase contains steam and CO_2, which are separated from each other by condensation. The final concentrated CO_2 stream is ready for CO_2 transport and storage.

As the most widely used solvent for CO_2 capture, MEA is still not an ideal solvent yet. Throughout the process, solvent degradation may take place in the presence of oxygen. Furthermore, secondary air emission is produced due to the

high volatility of the solvent. And its corrosivity and energy intensive regeneration result in high costs in capital and operation.

Improved amines, such as the secondary amines (e.g., DEA) and tertiary amines (e.g., MDEA) have been considered as an alternative for MEA. Primary and secondary amines react with CO_2 quickly to form carbamate through the zwitterion mechanism. For MEA, the corresponding heat of absorption is $Q = -\Delta H_R = 2.0\,\mathrm{MJ/kg} - CO_2$. The reaction of CO_2 with secondary amines has a lower enthalpy of reaction [54], which favors regeneration of the solvent by stripping.

Tertiary amines react with CO_2 following a base-catalyzed hydration mechanism, which is different from the zwitterion mechanism to form bicarbonate instead of carbamate. The overall reaction indicates a theoretical CO_2 loading capacity of 1 mol of CO_2 per mole of tertiary amine. However, the reactivity of tertiary amines with respect to CO_2 is lower than that of primary or secondary amines. The corresponding enthalpy of reaction for the bicarbonate formation is lower than that for the carbamate formation. This means lower energy consumption for solvent regeneration.

Piperazine (PZ) has been used in blended systems as an additive to increase the rate of absorption of CO_2 in systems with low absorption rates but otherwise attractive solvent characteristics [23]. Adding Piperazine into the solvent can improve the rate and capacity of CO_2 absorption by the following reactions.

$$KHCO_3 \rightarrow K^+ + HCO_3^- \tag{12.46}$$

$$PZ + HCO_3^- \leftrightarrow PZCOO^- + H_2O \tag{12.47}$$

$$PZCOO^- + HCO_3^- \leftrightarrow PZ(COO^-)_2 + H_2O \tag{12.48}$$

Reactions (12.47) and (12.48) also require low energy for regeneration. On the other hand, thermal degradation of Piperazine in CO_2 capture is a technical challenge that deserves further investigation.

An example of an optimized process for post-combustion CO_2 capture by amine scrubbing is available in the DOE-NETL report [19]. The CO_2 absorption rate of Piperazine (PZ) doubles that of 30 wt% MEA with 1.8 times the intrinsic working capacity. The incoming flue gas is cleaned by water spray to remove fine particulates and cooled down to 40–60 °C. Filtered lean solvent enters the amine scrubber, usually packed bed from upper level and flows downward by gravity to absorb CO_2 from the counter flow flue gas. Cleaned flue gas is further cold-water washed to recover the penetrating solvent droplets or vapor before discharging to the atmosphere through the stack. The washing water joins the lean solvent to form the rich solvent exiting the scrubber at the bottom of the tower. In addition to the main absorber, the process may also need SO_2 removal before the PZ absorber.

Recently, sterically hindered amines have also attracted considerable attention for their low regeneration costs. A sterically hindered amine is a primary amine where the amino group is attached to a tertiary carbon atom; it can also be a secondary amine where the amino group is attached to a secondary or tertiary

carbon atom. For example, 2-Amino-2-methyl-1-propanol (AMP) is a sterically hindered primary amine and 2-piperidineethanol (PE) is a sterically hindered secondary amines.

12.6.3 Non-amine-Based Chemical Absorption

12.6.3.1 Sodium Hydroxide-Based Chemical Absorption

The chemical reactions between CO_2 and sodium hydroxide can be described as follows:

$$CO_2 + H_2O \rightarrow H_2CO_3 \tag{12.49}$$

$$H_2CO_3 + NaOH \rightarrow NaHCO_3 + H_2O \tag{12.50}$$

$$NaHCO_3 + NaOH \rightarrow Na_2CO_3 + H_2O \tag{12.51}$$

Water and CO_2 first react to form carbonic acid, which reacts with sodium hydroxide to produce bicarbonate ($NaHCO_3$). Bicarbonate also reacts with sodium hydroxide to produce a more stable product of carbonate. There are $NaHCO_3$ and Na_2CO_3 in the final product. Their relative quantity depends on the pH of the liquid in the last two reactions.

Regeneration of NaOH is usually achieved by adding lime (CaO) into the final product converting Na_2CO_3 to $CaCO_3$, followed by calcination at 870 °C or higher to release the pure CO_2 for storage of other applications. The corresponding chemical reactions are

$$CaO + H_2O \rightarrow Ca(OH)_2 \tag{12.52}$$

$$Ca(OH)_2 + Na_2CO_3 \rightarrow 2NaOH + CaCO_3 \tag{12.53}$$

$$CaCO_3 \rightarrow CaO + CO_2 \tag{12.54}$$

The calcination reaction Eq. (12.54) is energy intensive and the corresponding enthalpy of reaction is about $\Delta H_R = 250\,\mathrm{kJ/mol\text{-}CO_2}$. It makes this process economically challenging. Alternatively, sodium hydroxide can be regenerated using sodium trititanate ($Na_2O \cdot 3TiO_2$), which requires half the energy for regeneration of NaOH.

12.6.3.2 Carbonate-Based Chemical Absorption

Limestone reacts with CO_2 and water as follows:

$$CO_2 + H_2O \rightarrow H_2CO_3 \tag{12.55}$$

$$CaCO_3 + H_2CO_3 \rightarrow Ca(HCO_3)_2 \tag{12.56}$$

These reactions take place in the processes that are used for power plant or cement plant flue gas cleaning. Usually crushed limestone is packed in a reactor and wetted by a continuous flow of water. The CO_2-laden flue gas is pumped through the reactor to enable the above chemical reactions.

Example 12.3:
How much water and $CaCO_3$ is needed to capture 1,000 kg of CO_2 from the flue gas? How much calcium bicarbonate $\left(Ca(HCO_3)_2\right)$ is produced?

Solution
By considering the following chemical reactions,

$$CO_2 + H_2O \rightarrow H_2CO_3$$

$$CaCO_3 + H_2CO_3 \rightarrow Ca(HCO_3)_2$$

the overall reaction formula is

$$CO_2 + H_2O + CaCO_3 \rightarrow Ca(HCO_3)_2$$

It indicates that the mole ratio of the compound in this reaction is 1:1:1:1. Therefore, in order to capture 1,000 kg of CO_2, which is (1000/44) kmole, the same mole amounts of $CaCO_3$ and water are consumed to produce the same mole amount of $Ca(HCO_3)_2$.

By considering their molar weight, the corresponding mass can be determined as: 2,300 kg of $CaCO_3$ 400 kg of water and 3,700 kg $Ca(HCO_3)_2$.

Unlike other processes, the bicarbonate-rich effluent stream can be disposed in the ocean instead of regeneration. It is environmentally beneficial in that it can counteract ocean acidification. The challenges are the (fresh) water consumption and the costs for transportation related to the feedstock and product disposal.

Alternatively, potassium carbonate (K_2CO_3) can be used as a regenerable chemical absorbent. The corresponding CO_2 absorption reactions are

$$K_2CO_3 + H_2O \rightarrow KOH + KHCO_3 \tag{12.57}$$

$$KOH + CO_2 \rightarrow KHCO_3 \tag{12.58}$$

These reactions are slow at low CO_2 partial pressure, although the regeneration of the absorbent can be achieved at relatively low desorption energy of about 0.9–1.6 MJ/kg-CO_2. Therefore, it is not recommended for post-combustion CO_2 capture.

12.6.3.3 Aqueous Ammonia-Based Chemical Absorption

An aqueous ammonia solution reacts with water and CO_2 to form ammonium carbonate and ammonium bicarbonate. The overall reaction can be described as follows:

$$NH_3 + CO_2 + H_2O \rightarrow NH_4HCO_3 \tag{12.59}$$

Ammonia based chemical absorption/scrubbing also can capture SO_2 and NO_2 from a flue gas. While it allows multiple air emission control, it is challenging to produce pure acidic gases. The best option is to use the ammonium salts as fertilizer feedstock.

A typical ammonia-based CO_2 capture process is as follows. In a counter flow absorption tower flue gas flows upward with aqueous ammonia downward. The absorption process operates at near-freezing conditions (0–10 °C) with the flue gas cooled by the upstream de-SO_2 process. The low temperature allows high absorption capacity and reduces ammonia evaporation, which is also called "*ammonia slip*."

Downstream the absorption tower, ammonia slip is further reduced by cold-water washing [39]. The effluent gas contains mainly nitrogen, oxygen and low-concentration penetrated CO_2. The solvent is regenerated at a temperatures of >120 °C pressures of >2 MPa. Cold-water washing is also employed to reduce ammonia slip in the generation process.

12.6.4 Ionic Liquids as CO_2 Solvents

Ionic liquids (ILs) have been developed for the physical and chemical absorption of CO_2. ILs are melting organic slats with unique properties. They comprise a large organic cation and a small inorganic anion. The use of ILs as CO_2 solvents is believed to have many advantages over conventional amine-based solvents, such as potentially lower energy consumption in the solvent regeneration step, lower volatility, lower vapor pressure, non-flammability, more thermally stable, and easier recycling. However, all these features are subjected to further R&D evaluation, and, they come with an unusually high manufacturing cost [9].

A great number of ILs have been developed and tested in laboratory. Among these ILs, the imidazolium class is the most widely investigated and reported. ILs

without functional groups can be used as physical sorbent for CO_2 capture. ILs prepared with specific function groups enable selective gas absorption. Amine functional groups have been used effective CO_2 chemical absorption.

After CO_2 sorption, the used ILs can be regenerated by heating the spent solvent to release the absorbed gas(es). Since regeneration usually takes place at a higher temperature than the sorption stage, thermal stability is a key factor in selecting the right ILs.

12.6.4.1 CO_2 Solubility in Physical Ionic Liquids

Earlier research on CO_2 capture with ILs focused primarily on physical absorption without chemical reactions. In this section we concentrate on properties that affect the CO_2 physical absorption including CO_2 solubility and selectivity.

The actual mechanisms behind the high CO_2 solubility in IL are still not well understood [49]. Scientists and engineers are actively working on understanding and increasing the solubility of CO_2 in ILs. A review of the different approaches that have been used to model the phase behavior of gas-IL systems is provided by Vega et al. [55]. Molecular simulation and experimental data have shown that anion and cation play an important role in the dissolution of CO_2 [6, 11]. Most researchers agree that the anion dominates the solubility of CO_2 in an IL and that the cation plays a secondary role. Nonetheless, anion-fluorination and cation-fluorination can improve the solubility much [3].

CO_2 solubility in ILs increases with increasing molecular weight, molar volume, and the free volume of ILs. CO_2 solubility in ILs is dominated by entropic effects rather than solute–solvent interactions [12]. As such, it cannot be calculated based on mole fraction (like in Henry's law or Raoult's law in Sect. 2.3) because of the strong molecular weight (molar volume) of ILs. It should be determined as a function of molality, that is, the mole amount of solubility per kilogram of solvent (mole CO_2/kg IL).

Before more sound theories are available, we can use the following empirical correlation proposed by Carvalho and Coutinho [12] to calculate the CO_2 solubility in ILs by physical absorption:

$$P = m_i^0 \times \exp\left(6.8591 - \frac{2004.3}{T}\right) \tag{12.60}$$

where m_i^0 is the molality in (mole of CO_2/kg of IL), P is the pressure in MPa, and T is temperature in K. This equation was obtained using experimental data and is deemed valid for pressures up to 5 MPa, molalities up to 3 mol/kg, and temperatures ranging from room temperature to 363 K. Figure 12.7 shows the calculated solubility versus pressure at three different temperatures. For a fixed temperature, the solubility is in linear relationship with the pressure.

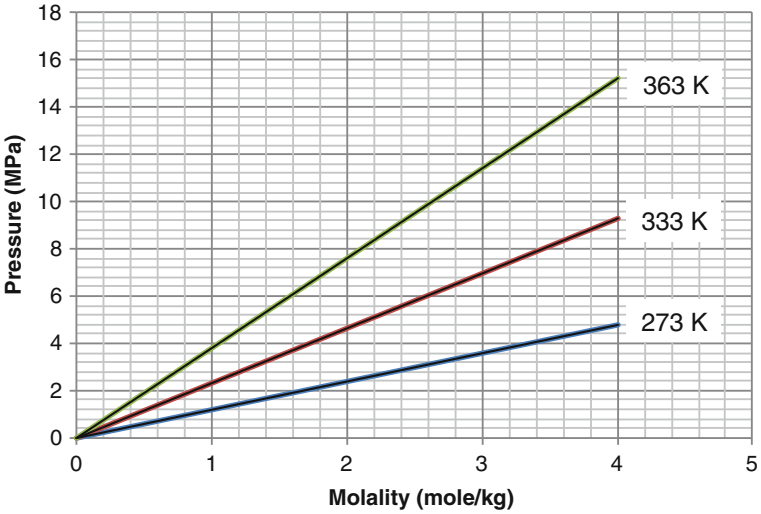

Fig. 12.7 CO_2 solubility in physical ionic liquids

Example 12.4: CO_2 solubility in physical IL
Estimate the amount of CO_2 in kg that can be absorbed into 1,000 kg of IL at 2 MPa and 300 K using the Carvalho and Coutinho [12] model.

Solution
From Eq. (12.60) we can get

$$m_i^0 = \frac{P}{\exp\left(6.8591 - \frac{2004.3}{T}\right)} = \frac{2}{\exp\left(6.8591 - \frac{2004.3}{300}\right)} = 1.6742(\text{mole } CO_2/\text{kg IL})$$

The molar weight of CO_2 is 44 g/mole, and that gives the solubility as

$$c_{CO_2} = 1.6742 \times 0.044(\text{kg } CO_2/\text{kg IL}) = 0.07357(\text{kg } CO_2/\text{kg IL})$$

As seen in the result of this example, CO_2 solubility is low in ILs, which means extremely high cost is needed to use ILs to absorb CO_2 from industrial sources.

12.6.4.2 Gas Selectivity

Another important indicator of the right adsorbent is its selectivity from a gas mixture. Since there are always other gases, more or less, present besides CO_2. CO_2 selectivity affects the performance of CO_2 adsorption into ILs. Therefore, CO_2

Table 12.8 Henry's law constants of different gases in [hmpy][Tf_2N] ionic liquid

Gas	Temperature	
	283 K	298 K
SO_2		1.54 ± 0.01
CO_2	25.4 ± 0.1	32.8 ± 0.2
CH_4		300 ± 30
O_2	422 ± 220	463 ± 104
N_2		3390 ± 2310

solubility along is not sufficient to judge the separation performance of a solvent. We must also consider selectivity.

For pre- and post-combustion CO_2 capture, we are mostly concerned with the selectivity of CO_2/H_2, CO_2/CH_4 and CO_2/N_2. Depending on the actual gas compounds, selectivity like CO_2/H_2S, CO_2/SO_x, H_2S/CH_4 and CO_2/CO might also become important.

Ramdin et al. [49] summarized the scarce selectivity data reported in the literature. Anderson et al. [4] reported the solubility of different gases in different ILs in terms of Henry's law constant. Table 12.8 shows the Henry's law constants of [hmpy][Tf_2N]. In general, N_2 and O_2 solubility are lower compared to CO_2 leading to a high CO_2/N_2 or CO_2/O_2 selectivity.

On the other hand, SO_2 is very competitive to CO_2 absorption; SO_2 should be removed from stream first before carbon capture.

12.7 CO_2 Transportation

While CO_2 capture is accomplished at the source of emission, its destination storage sites are usually far away from the source. Transportation infrastructure is necessary to deliver CO_2 from one point to another. Although other options like rail and trucking have been studied at small scales, realistic CO_2 transportation technologies for large-scale CO_2 delivery are

- Pipeline transportation
- Ship transportation

Transporting CO_2 via pipeline is deemed to be cost-effective on land, whereas ship transportation is more economical when there is a large body of water between the source and destination. For either case, transported CO_2 is not a gas but a liquid.

12.7.1 Pipeline Transportation

Prior to transportation via pipeline, CO_2 is compressed to a supercritical fluid or liquid state for efficient pipeline transportation [51]. The critical point of CO_2 is 31.1 °C and 73 atm. However, temperature and pressure drops along the pipeline, therefore, prior to delivery CO_2 is compressed to a pressure that is more than 73 atm.

The pressure drop per unit length of pipeline can be described as

$$\frac{\Delta P}{\Delta L} = f_D\left(\frac{\rho U^2}{2d}\right) \tag{12.61}$$

where $\frac{\Delta P}{\Delta L}$ is the pressure drop per unit length of pipeline (Pa/m), f_D is the dimensionless Darcy friction factor, d is the diameter of the pipeline, ρ is the density of the fluids, CO_2 in this case, and U is the average speed of the fluid.

The Darcy friction factor can be calculated using the Colebrook-White equation [14].

$$f_D^{-1/2} = -2\log_{10}\left(\frac{\varepsilon}{3.7d} + \frac{2.51}{\mathrm{Re}f_D^{1/2}}\right) \tag{12.62}$$

where ε is the pipeline inner surface roughness, which is about 46 μm, for typical commercial steel pipes. Re is the Reynolds number in pipeline and it can be calculated using Eq. (12.63)

$$\mathrm{Re} = \frac{\rho U d}{\mu} = \frac{4\dot{m}}{\mu\pi d} \tag{12.63}$$

Example 12.5: Pressure drop in a pipeline
Consider a pipeline made of commercial steel with an inner diameter of 40 cm for transporting CO_2 at a flow rate of 3.5 Mega tons per year. Use CO_2 properties under 11 MPa and 25 °C as follows: $\rho = 877\,\mathrm{kg/m^3}$ and $\mu = 7.73 \times 10^{-5}\,\mathrm{Pa \cdot s}$. Estimate the pressure drop over a distance of 100 km.

Solution
Convert the unit of the CO_2 flow rate as

$$\dot{m} = 3.5\frac{\mathrm{Mt}}{\mathrm{year}} = \frac{3.5 \times 10^6 \times 1000\,\mathrm{kg}}{365 \times 24 \times 3600\,\mathrm{s}} = 111\,\mathrm{kg/s}$$

The average speed in the pipe can be determined using

$$U = \frac{4\dot{m}}{\rho\pi d^2} = \frac{4 \times 111}{877 \times \pi \times 0.4^2} = 1.007\,\text{m/s}$$

The corresponding Reynolds number is determined using Eq. (12.63).

$$\text{Re} = \frac{4\dot{m}}{\mu\pi d} = \frac{4 \times 111}{7.73 \times 10^{-5} \times \pi \times 0.4} = 4.57 \times 10^6$$

With $\varepsilon = 4.6 \times 10^{-5}$ m, $d = 0.4$ m and $\text{Re} = 4.57 \times 10^6$, the Darcy friction factor can be determined using Eq. (12.62) as follows:

$$\begin{aligned} f_D^{-\frac{1}{2}} &= -2\log_{10}\left(\frac{\varepsilon}{3.7d} + \frac{2.51}{\text{Re}f_D^{\frac{1}{2}}}\right) \\ &= -2\log_{10}\left(\frac{4.6 \times 10^{-5}}{3.7 \times 0.4} + \frac{2.51}{4.57 \times 10^6 f_D^{\frac{1}{2}}}\right) \\ &= -2\log_{10}\left(3.108 \times 10^{-5} + \frac{5.492 \times 10^{-5}}{f_D^{\frac{1}{2}}}\right) \end{aligned}$$

By iteration, we can get $f_D = 0.0217$.

Then we can calculate the pressure drop over 100 km distance length using Eq. (12.61).

$$\begin{aligned} \Delta P &= f_D\left(\frac{\rho U^2}{2d}\right)\Delta L \\ &= 0.0217\left(\frac{877 \times 1.007^2}{2 \times 0.4}\right) \times 100 \times 10^3 = 2.41 \times 10^6\,\text{Pa} \end{aligned}$$

So the pressure drop is about 2.41 MPa over a distance of 100 km. Due to this kind of great resistance, intermediate pumping (or booster) stations are required at certain intervals along the pipeline.

We have to be careful that the CO_2 properties are assumed constant in the above example in order to simplify the calculation. In reality, they cannot remain constant. Glilgen et al. [25] experimentally determined the pressure, density, and temperature relationship of CO_2 in the homogeneous region for pressures up to 13 MPa and temperatures in the range of 220–360 K. For $P < 9$ MPa and $T > 298$ K, CO_2 density varies considerably with P and T.

In the engineering practice, it is critical to ensure enough pressure to maintain above vapor–liquid equilibrium conditions to avoid liquid slugs and other operational problems resulted from a two-phase (gas–liquid) flow. A typical operating

pressure is in the range of 84.9–207.3 atm where CO_2 is a dense-phase fluid over a wide range of temperatures. Nonetheless, the gas properties also depend on impurities such as SO_x, NO_x, and other air contaminants. A complex model is required to accurately predict the fluid property along the pipeline. Interested readers have to dig deeper into the literature for in-depth knowledge.

12.7.2 Ship Transportation

For CO_2 transport by ship, it is most efficient to transport CO_2 as a cryogenic liquid. The best condition for CO_2 transport by ship is about 6.4 atm and −51.2 °C [7]. As it is stored in containers during transportation, there is no pressure drop concern.

The optimal transport pressure depends on the state of the fluid. In short, large-scale transport of CO_2 by ship could be achieved by semi-pressurized vessels of around 20,000 m^3 at pressures of 6.415 atm and −52 °C in order to use existing ship and infrastructures. This condition also allows low unit cost in transport. The total costs of ship-based transport are estimated to be $20–30 per ton CO_2.

12.8 CO_2 Storage

It would be ideal to convert CO_2 into valuable products, such as methanol. A small portion can be used for production of soda drinks. Unfortunately, applications and consumptions of CO_2 are very limited compared to its production rate in fossil fuel-fired power plants and vehicles.

More practically, the captured CO_2 must be then stored properly without escape from its sinks into the atmosphere. Options listed below are considered relatively feasible both economically and environment-friendly.

(1) Geological storage

- Enhanced oil recovery (EOR),
- Deep saline reservoirs and aquifers,
- Unmineable coal beds.

(2) Deep ocean storage
(3) Ecosystem storage

Geological storage is the only CO_2 storage method that has been well developed globally at a commercial scale. Ocean storage is under extensive research and development owing to its potentially large capacity. Ecosystem storage is another promising approach that is under investigation. These options are introduced as follows.

12.8.1 Enhanced Oil Recovery and Enhanced Gas Recovery

Carbon dioxide (CO_2) can be employed for EOR by CO_2 flooding for reservoirs deeper than 800 m. This depth allows CO_2 to be stored as a dense supercritical fluid. In the EnCana Weyburn field project that started September 2000, for example, over 2.2 Mt supercritical CO_2 per year is injected to a depth of 1,400–1,500 m for OER [22].

A schematic diagram of an EOR process is shown in Fig. 12.8. CO_2 is injected into the deep reservoir from the injection well, and it forms a CO_2 bank. A CO_2 miscible oil bank is formed as a result of the miscible CO_2-oil mixing. The mixture of CO_2 and crude oil is delivered to the ground surface through the production well. They are separated at the ground facilities, producing liquid and gaseous fuels with recovered CO_2.

For immiscible CO_2 operation, CO_2 bank pushes oil forward from the reservoir to the production well. Depending on the reservoir, the incremental oil recovery by EOR ranges from 5 to 15 %. This additional economic benefit makes EOR competitive over other options.

Eventually, a significant amount of CO_2 injected for EOR is trapped underground by residual oil, water, or mineral. It is expected that this part of CO_2 can remain underground for thousands of years. However, the supercritical CO_2 is mixed with water may be transported underground out of the reservoirs. Long term CO_2 distribution in the reservoirs can be predicted by numerical simulations for long-term risk assessment.

Similar to EOR, CO_2 can also be injected into depleting gas reservoir for enhanced gas recovery. However, the economical return is not as high as EOR in that most primary gas recovery rate is pretty high already, and current gas price is low.

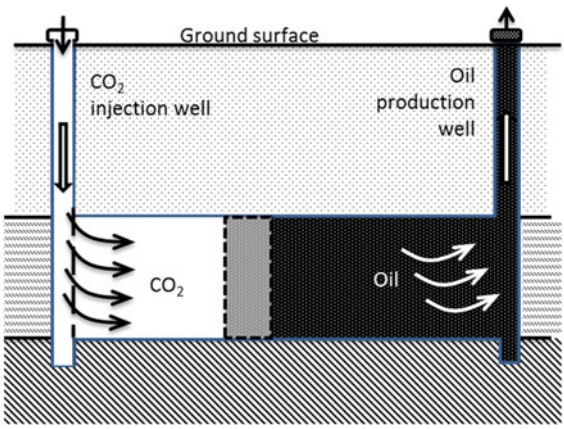

Fig. 12.8 EOR by CO_2 injection

12.8.2 Coal Bed Methane Recovery

Coal bed methane is the methane adsorbed in underground coals. Coal bed methane recovery is then a methane desorption process based on pressure swing desorption. The process is similar to EOR above; liquefied CO_2 is injected into a deep well, which is drilled into the coal bed, to reduce the hydrostatic pressure. As a result, methane is released from coal bed and transported to gas pipeline.

CO_2 injection also results in enhanced methane recovery from coal bed methane by the competitive adsorption between CO_2 and methane. According to physical adsorption mechanisms, CO_2 and methane compete for the adsorption sites in the pores of the coal. As seen Fig. 12.9, coal adsorbs CO_2 more effectively than methane [37], this adsorption preference results in desorption of methane from the coal when CO_2 is injected into the coal bed. Liberated methane from the coal bed is also delivered to the surface facilities.

Meanwhile, the replacement of methane with CO_2 on the pores of the coal also results in swelling of the coal matric and this may lead to reduced permeability, and consequent coal softening and more CO_2 injection in order to recover more methane.

Cost-effective coal bed methane recovery requires high initial concentration of methane and adequate permeability for gas flow. Both depend on the pressure or depth of the coal bed: the deeper, the higher methane concentration but the lower permeability. This contradictory effect requires economical coal bed methane recovery to be executed at a depth in the range of 300–1,000 m or so.

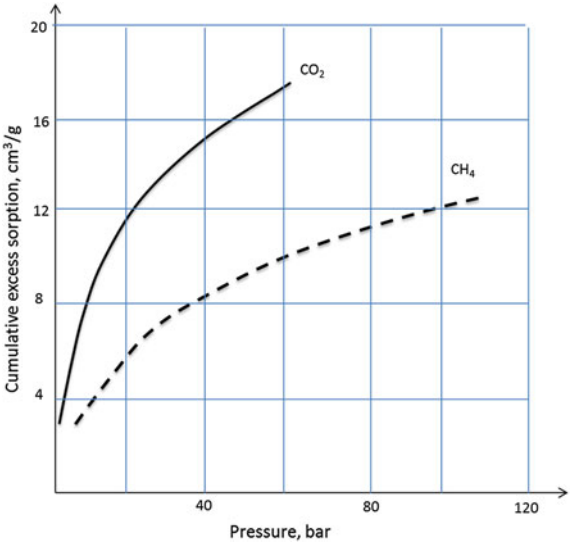

Fig. 12.9 Excess sorption isotherms of CO_2 and CH_4 in a coal (*Data source* Krooss et al. [37])

12.8.3 Saline Aquifer Storage

Saline aquifer storage is a CO_2 storage option for regions without energy resources recovery opportunities [13, 53]. Similar to EOR, CO_2 is injected into the saline aquifer as a supercritical fluid, which forms a deeply underground plume. The storage potential and security risks depend on the geological characteristics and usually they are predicted by model simulations.

Figure 12.10 shows a schematic diagram of deep saline aquifer CO_2 storage. CO_2 is injected down to the underground and sealed with a cap rock. Over time, stored CO_2 migrates slowly out of the CO_2 reservoir as a result of dissolution or chemical reactions with the cap rock.

There are four primary mechanisms for saline aquifer CO_2 storage, in order of increasing security

- Structural and stratigraphic trapping
- Residual trapping
- Solubility trapping, and
- Mineral trapping

Structural and stratigraphic trapping CO_2 is trapped under a cap rock. This is simply an initial and temporary physical trapping of CO_2 for 1–100 years, depending on the structural characteristics.

Residual trapping As the CO_2 plume rises through a water-saturated rock, high pressure buoyant CO_2 drives water out of the pores of the rock. Some CO_2 is trapped in the rock pores as residue. The residual trapping over time declines as CO_2 is dissolved in the formation brine and diffuses into the surrounding unsaturated aquifer.

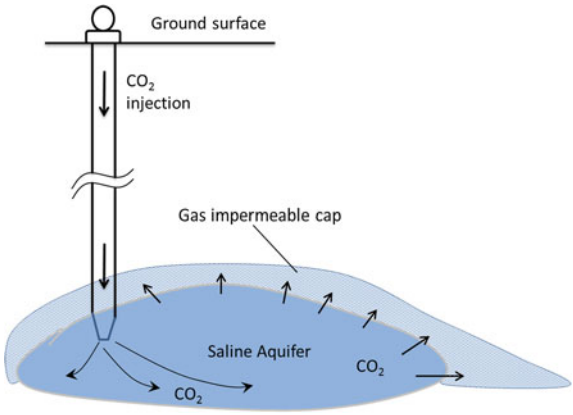

Fig. 12.10 Saline aquifer CO_2 storage

According to Darcy's law, the volume flow rate of a fluid through the porous medium is

$$J = -\frac{kA}{\mu}\frac{\mathrm{d}p}{\mathrm{d}x} \tag{12.64}$$

where J is the volume flow rate in m^3/s, k is he permeability of the porous medium (m^2), A is the area (m^2), μ is the fluid viscosity (kg/m · s or Pa · s), $\mathrm{d}p/\mathrm{d}x$ stands for the pressure gradient in Pa/m over flow direction. One can estimate the bottom hole pressure corresponding to a certain CO_2 injection rate or leaking rate.

Solubility trapping Solubility trapping is one major trapping mechanism in saline aquifer storage of CO_2. Dissolution of CO_2 in formation water can last as long as 1,000 years, depending on the brine composition and pH as well as the mineralogy of the reservoir.

Mineral trapping Mineral trapping is resulted from the chemical reactions between CO_2 and metal ions such as Ca^{2+}, Fe^{2+} and Mg^{2+}, which are rich in the surrounding rocks. As the carbonates produced precipitate in the rock pores the reactions slow down over time. As a result, it takes 10–10,000 years to saturate the pores. Meanwhile, the chemical reactions take place in the pores of the cap rock, improving the integrity of cap rock over time.

12.8.4 Deep Ocean Storage

The ocean naturally traps over 143,000 Gt of CO_2, which is 50 times more than that in the atmosphere. The uptake of CO_2 in ocean has been increasing over the past centuries as a result of the increasing atmospheric CO_2 concentration. However, it still can hold much more! A comprehensive documentation of deep ocean CO_2 storage is given by Caldeira et al. in the form of a SRCSS Special Report to IPCC [32] (Chap. 6, Ocean Storage).

Similar to what was introduced in mass transfer in absorption (Sect. 2.3.4), natural CO_2 storage in ocean is a chemical absorption process. CO_2 enters ocean through the surface water, where the equilibrium concentration is governed by Henry's law, $x_{CO_2} = P_{CO_2}/\mathrm{H}$, where H is the Henry's law constant for CO_2 -sea water system.

The solubility of CO_2 in seawater is not constant everywhere; it depends on the pressure, salinity, pH, and temperature of seawater.

Deeper into the ocean, CO_2 goes through chemical reactions. Several simplified chemical equilibriums define the process as

$$CO_2 + H_2O \leftrightarrow H_2CO_3 \leftrightarrow HCO_3^- + H^+ \leftrightarrow CO_3^{2-} + 2H^+ \tag{12.65}$$

All these species are grouped as dissolved inorganic carbon (DIC). H_2CO_3 also reacts with dissolved limestone in the ocean, which is a result of weathering the earth surface, and the simplified chemical reaction is

$$CaCO_3 + H_2CO_3 \rightarrow Ca^{2+} + 2HCO_3^- \tag{12.66}$$

Besides the inorganic carbons, CO_2 is also converted into particulate organic carbon (POC) and fertilizer by photosynthesis. For example,

$$6CO_2 + 6H_2O + uv \rightarrow C_6H_{12}O_6 + 6O_2 \tag{12.67}$$

$$106CO_2 + 122H_2O + 16HCO_3^- + H_3PO_4 \rightarrow C_{106}H_{263}O_{110}N_{16}P + 138O_2 \tag{12.68}$$

One way or another, CO_2 is not saturated in deep ocean as a result of these chemical reactions and biological conversions of CO_2 into organic and inorganic carbon compounds. Therefore, more CO_2 can be stored in deep ocean. However, natural absorption of CO_2 into ocean is a slow process and it cannot catch up with the increase rate of anthropogenic CO_2 in the atmosphere.

This process can be expedited by injecting CO_2 into deep ocean. Based on the properties of liquid CO_2 in ocean, engineered deep ocean CO_2 storage can be achieved by

- direct CO_2 dissolution, and
- liquid CO_2 isolation

The fate of the injected CO_2 depends on the injection depth in the ocean. At a depth of about 500 m (corresponding to the pressure of 4–5 MPa and temperatures in the range of 0–10 °C), CO_2 starts to liquefy and the liquid CO_2 has a density of 860–920 kg/m^3. The deeper into the ocean, the greater liquid CO_2 density as a result of the greater pressure.

According to the liquid CO_2 density relative to the seawater density, the depths can be divided into three zones where CO_2, floats, suspends, and sinks, respectively. As shown in Fig. 12.11, liquid CO_2 density is close to that of seawater at depths of about 2,500–3,000 m. This is also referred to as thermocline. Above this zone, CO_2 density is less than the surrounding seawater. Therefore, the liquid CO_2 droplets rise as a plume. In the transition zone, CO_2 density is nearly close to that of seawater and it suspends in seawater due to neutral buoyance. Further deep into the ocean, CO_2 density surpasses that of the seawater resulting in sinking CO_2 plume. For any one of the three scenarios, most of the released CO_2 will eventually dissolve in the ocean.

The sinking CO_2 droplets eventually reach the bottom of the ocean enabling liquid CO_2 isolation as a liquid lake in an ocean floor depression. Such a CO_2 lake can be made by injecting liquid CO_2 to the ocean floor depression or releasing CO_2 at a depth that is close to the target lake. Settled liquid CO_2 in the lake mixes with

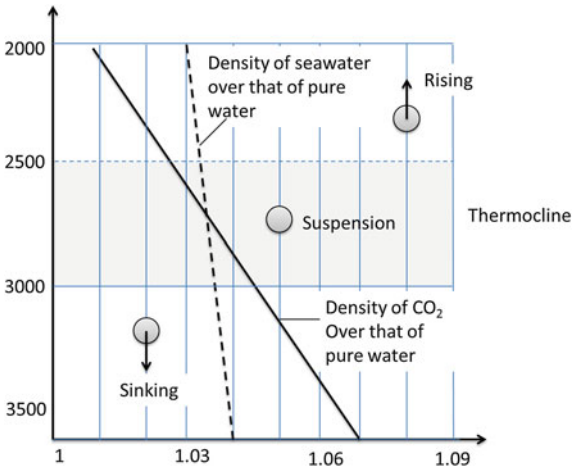

Fig. 12.11 CO_2 density versus ocean depth

the capping sea water due to ocean turbulence. This vertical mixing results in certain amount of CO_2 dissolution. Undisturbed CO_2 lake is expected to have a lifetime of about 10,000 years.

12.8.5 Ecosystem Storage

Like extraterrestrial oceans, terrestrial ecosystems have been an important and long-lasting natural CO_2 sink by photosynthetic reactions in biomass and complex interactions with soils. Unfortunately, recent human activities have reduced its CO_2 storage capacity resulting in increased atmospheric CO_2 concentration. Before the availability of other cost-effective options, ecosystem CO_2 storage is deemed to have a potential to buy human more time and slow down the negative impact of increasing anthropogenic CO_2 emissions.

While the CO_2 storage capacity of terrestrial ecosystems is much less than that of the ocean, it is easy to operate and cost-effective. Ecosystem carbon storage can be achieved by

- Agricultural carbon storage
- Change in land use
- Energy crops production.

12.8.5.1 Agricultural Carbon Storage

Agricultural carbon storage is an approach to additional CO_2 storage in biomass by improved management of vegetation and soil in the ecosystem. Specifically, it can

be achieved by conservation tillage, crop selection, rotation and intensified cropping, managing soil biogeochemistry, and manipulation of microbial communities.

Tilling disturbs the soil resulting in reduced CO_2 storage. Therefore, reduced tillage intensity contributes to increased CO_2 storage. It can be achieved by no till, ridge till, minimum till, and mulch till. Conservation tillage aims at the reduction of soil erosion and the maintenance of water-holding capacity of soils. It is expected to restore the loss of CO_2 that was released by historical intensive tillage practice over a short period of time.

Crop selection, rotation, and intensified cropping allow more above-ground biomass, and consequently enable more CO_2 storage. Their net carbon storage effects will be maximized when applied in conjunction with conservation tillage.

Soil organic carbon may depend on the soil biological and chemical properties, for example, pH. Addition of metal oxides such as CaO and MgO is expected to enhance the chemical sorption of CO_2 into the soils. However, this change in pH may also change the behaviors of microorganisms in the soils.

Fungal and bacterial species in the soils play an important role in the release and storage of soil organic carbon as well as the emissions of other GHGs such as N_2O and CH_4. The complexity of microbial community opens another opportunity for potential CO_2 storage and/or reduced GHG emissions by multiplication of the microbial species. Different ongoing research projects are being conducted to evaluate the feasibility of this approach.

12.8.5.2 Change in Land Use

Land on the earth can be grouped into, in the increasing order of carbon storage share, degraded land < croplands < pasture < grass lands < wetlands < forest. Land upgrading in terms of carbon storage capacity is expected to contribute to additional CO_2 storage. IPCC (2000) report on land use, land-use change and forestry estimated that about 1 Gt-C per year could be stored in the short term as a result of the regrowth of perennial vegetation and improvements of land management practices in croplands, grasslands, and forests. For example, change in land use can be achieved by wetland management and restoration and forestry management, afforestation, and reforestation.

Protection and restoration of wetlands presents an opportunity for increased underground organic carbon storage. The residence time of the CO_2 stored in wetland depends on the plant type and the degree of inundation. Since wetland is the second best land in terms of CO_2 storage, only after forest, more CO_2 is released into the atmosphere when wetland is drained for uses as agricultural or urban and industrial development. Unfortunately, recent research shows that it is challenging to restore the lost CO_2 simply by recreating wetlands. More research and development is needed in this area.

The loss of CO_2 storage in forest can be reduced by reducing logging and deforestation. Protection of old trees and regeneration of secondary and degraded

forests stand biomass with improved CO_2 storage. Afforestation of croplands is another option at a reasonable cost. The effect can be further extended by replacing soft bushes with standing wood forest.

12.8.5.3 Energy Crop Production

Energy crop production is the option that regenerates biomass from CO_2 in the atmosphere or concentrated CO_2 from carbon capture CO_2 is converted into biomass by photosynthesis and these crops are burned or converted into fuels for combustion, where CO_2 is released again. Energy crops are plants grown specifically for energy production. They are planted and harvested periodically. These energy crops contain oils (soybeans, nuts and grains), sugar (sugar beets), starches (corns, cereal), and lignocellulose in residues or woody biomass.

Technical description of energy production and biofuels from energy crops have been introduced in Sect. 8.4. It is not repeated here.

Energy crops can be classified into herbaceous and short-rotation woody crops [10]. The former is characterized with low lignin content enabling easy delignification and improved accessibility to carbohydrate in lignocellulose for biofuel production. Examples of herbaceous energy crops are

- Perennials like sugarcane, napier grass
- Annuals such as corn, forage sorghum
- Thin-stemmed, warm season perennial, e.g., switch grass

Woody energy crops are fast growing and suitable for use in dedicated supply systems. Desirable candidates are characterized with rapid juvenile growth, wide site adaptability, and pest and disease resistance. They are grown on a sustainable basis and harvested on a rotation of 3–10 years. For example,

- Flowering plants like willow, oak, poplar
- Evergreens like pine, spruce, cedar

Algal biomass is a special energy crop that can be grown in an aqueous environment. It can be cultivated in ponds built beside stationary CO_2 capture sources such as power plants, cement plants, and municipal waste plants. This practice enables high productivity per area of land with low foot prints. In addition, it is expected to produce and harvest biomass continuously with engineered nutrient control. The process allows simple operation with low quality land and water that are unsuitable for other crop growth. Processed algae can be used as a solid fuel or a feedstock for biodiesel. Readers are referred to the literature for advances in algae and energy crop production.

12.9 Environmental Assessment

Although many technologies have been claimed to be effective in reducing carbon emissions, a comprehensive life cycle analysis (LCA) must be conducted before an affirmative conclusion can be made. Since the 1970s, environmental assessment has been developed as a systematic process to identify, analyze, and evaluate the environmental effects of products or activities to ensure that the environmental implications of decisions are taken into account *before* the decisions are made. Environmental assessment allows effective integration of environmental considerations and public concerns into decision-making.

In principle, environmental assessment can be undertaken for individual projects such as a dam, motorway, factory, or a bioenergy plantation; it can also be done at a large scale for plans, programs, and policies. These approaches aim at providing a systematic procedure for identifying potential risks to human health and the environment, and a comparison of the respective risks to alternative options for different environmental compartments (air, soil, water).

LCA is a specific method developed in the 1980s for determining and comparing the potential environmental impacts of product systems or services at all stages in their life cycle—from extraction of resources, through the reduction and use of the product to reuse, recycling or final disposal. It can be applied in strategy formulation, product development, and marketing. The LCA methodology has been developed extensively during the last decade. Moreover, a number of LCA-related standards (ISO 14040-14043) and technical reports have been published by the International Organization for Standardization (ISO) to streamline the methodology.

The LCA approach is quite data-intensive. Not only are direct impacts included, but also those stemming from "upstream" activities such as mining, processing, and transport, as well as the materials (and energy) needed to manufacture all processes. With LCA being developed as a specific assessment methodology to compare products, the formal assessment requirements from the ISO standards for LCA are demanding with regard to time and resources.

References and Further Readings

1. Aboudheir A, Tontiwachwuthikula P, Chakmab A, Idema R (2003) Kinetics of the reactive absorption of carbon dioxide in high CO_2-loaded, concentrated aqueous monoethanolamine solutions. Chem Eng Sci 58(2003):5195–5210
2. Adanez J, Abad A, Garcia-Labiano F, Gayan P, de Diego LF (2012) Progress in chemical-looping combustion and reforming technologies. Prog Energy Combust Sci 38:215–282
3. Almantariotis D, Gefflaut T, Padua AAH, Coxam JY, Costa Gomes MF (2010) Effect of fluorination and size of the alkyl sidechain on the solubility of carbon dioxide in 1-alkyl-3-methylimidazolium bis(trifluoromethylsulfonyl)amide ionic liquids. J Phys Chem B 114:3608–3617

4. Anderson JL, Dixon JK, Brennecke JF (2007) Solubility of CO_2, CH_2, C_2H_6, C_2H_4, O_2 and N_2 in 1-hexyl-3-methylpyridinium bis (trifluoromethylsulfonyl)imide: comparison to other ionic liquids. Acc Chem Res 40:1208–1216
5. Anderson DM, Mauk EM, Wahl ER, Morrill1 C, Wagner AJ, Easterling D, Rutishauser T (2013) Global warming in an independent record of the past 130 years. Geophys Res Lett 40 (1):189–193
6. Anthony JL, Anderson JL, Maginn EJ, Brennecke JF (2005) Anion effects on gas solubility in ionic liquids. J Phys Chem B 109:6366–6374
7. Aspelund A, Mølnvik MJ, de Koeijer G (2006) Ship transport of CO_2 technical solutions and analysis of costs, energy utilization, exergy efficiency and CO_2 emissions. Chem Eng Res Des 84(A9):847–855
8. Bidwe AR, Mayer F, Hawthorne C, Charitos A, Schuster A, Schenecht G (2011) Use of ilmenite as an oxygen carrier in chemical looping combustion-batch and continuous dual fluidized bed investigation. Energy Procedia 4:433–440
9. Boot-Handford ME et al (2014) Carbon capture and storage update. Energy Environ Sci 7:130–189
10. Brown RC (2003) Biorenewable resources, engineering new products from agriculture. Blackwell Publishing, Iowa State Press, Boston
11. Cadena C, Anthony JL, Shah JK, Morrow TI, Brennecke JF, Maginn EJ (2004) Why is CO_2 so soluble in imidazolium-based ionic liquids? J Am Chem Soc 126:5300–5308
12. Carvalho PJ, Coutinho JAP (2010) On the nonideality of CO_2 solutions in ionic liquids and other low volatile solvents. J Phys Chem Lett 1:774–780
13. Chadwick RA, Zweigel P, Gregersen U, Kirby GA, Holloway S, Johannessen PN (2004) Geological reservoir characterization of a CO_2 storage site: the Utsira Sand, Sleipner, northern North Sea. Energy 29:1371–1381
14. Colebrook CF (1939) Turbulent flow in pipes, with particular reference to the transition region between smooth and rough pipe laws. J Inst Civil Eng 11(4):133–156
15. Cuadrat A, Abad A, Garcıa-Labiano F, Gayan P, de Diego LF, Adanez J (2012) Effect of operating conditions in chemical-looping combustion of coal in a 500 Wth unit. Int J Greenhouse Gas Control 6:153–163
16. Danckwerts PV (1979) The reaction of CO_2 with ethanolamines. Chem Eng Sci 34:443–446
17. D'Alessandro DM, Smit B, Long JR (2010) Carbon dioxide capture: prospects for new materials. Angew Chem Int Ed 49(35):6058–6082. doi:10.1002/anie.201000431
18. DOE-NETL (2011) Research and development goals for CO_2 capture technology; Pittsburgh, PA, DOE/NETL-2009/1366
19. DOE-NETL (2012) Techno-economic analysis of CO_2 capture-ready coal-fired power plants, DOE/NETL-2012/1581
20. de Nevers N (2000) Air pollution control engineering. The McGraw-Hill Companies, Inc, New York
21. EIA (Energy Information Administration) (2007) International Energy Outlook (IEO), May 2007
22. EIA (2014) EIA.doe.gov. http://www.eia.gov/oiaf/1605/ggccebro/chapter1.html. Accessed 17 June 2014
23. Freeman S, Davis J, Rochelle GT (2010) Degradation of aqueous piperazine in carbon dioxide capture. Int J Greenhouse Gas Control 4:756–761
24. Grande CA (2012) Advances in pressure swing adsorption for gas separation. ISRN Chem Eng 2012, Article ID 982934. doi:10.5402/2012/982934
25. Glilgen R, Klenrahm R, Wagner W (1992) Supplementary measurements of the (pressure, density, temperature) relation of carbon dioxide in the homogeneous region at temperatures from 220 K to 360 K and pressures up to 13 MPa. J Chem Thermodyn 24:1243–1250
26. Houghton JT et al (eds) (1996) Climate change 1995: the science of climate change, IPCC. Cambridge University Press, Cambridge
27. Houghton J (1997) Global warming: the complete briefing, 2nd edn. Cambridge University Press, Cambridge

28. Houghton JT, Jenkins GJ, Ephramus JJ (eds) (1990) Climate change: the IPCC science assessment. Cambridge University Press, Cambridge
29. Houghton RA, Woodwell GM (1989) Global climate change. Sci Am 260(4):36–44
30. IPCC (The Intergovernmental Panel on Climate Change) (2005) Carbon capture and sequestration report
31. IPCC (2007) Changes in atmospheric constituents and in radiative forcing of the 2007. IPCC Fourth Assessment Report (AR4) by Working Group 1 (WG1). http://www.ipcc.ch/pdf/assessment-report/ar4/wg1/ar4-wg1-chapter2.pdf
32. IPCC (2013) Climate change 2013. In: Solomon S, Qin D, Manning M, Marquis M, Averyt K, Tignor MMB, Miller HL Jr, Chen Z (eds) The physical science basis. Cambridge University Press, New York
33. Ishida M, Zheng D, Akehat T (1987) Evaluation of a chemical-looping-combustion power-generation system by graphic exergy analysis. Energy 12(2):147–154
34. Jerndal E, Mattisson T, Lyngfelt A (2006) Thermal analysis of chemical-looping combustion. Chem Eng Res Des 84:795–806
35. Kim YE, Lim JA, Jeong SK, Yoon YI, Bae ST, Nam SC (2013) Comparison of carbon dioxide absorption in aqueous MEA, DEA, TEA, and AMP solutions. Bull Korean Chem Soc 34 (3):783–787
36. Ko J, Li M (2000) Kinetics of absorption of carbon dioxide into solutions of N-methyldiethanolamine + water. Chem Eng Sci 55:4139–4147
37. Krooss BM, van Bergen F, Gensterblum Y, Siemons N, Pagnier HJM, David P (2002) High-pressure methane and carbon dioxide adsorption on dry and moisture-equilibrated Pennsylvanian coals. Int J Coal Geol 51:69–92
38. Lewis WK, Gilliland ER (1954) US Pat., No. 2,665,972
39. Li K, Yu H, Tade M, Feron P, Yu J, Wang S (2014) Process modeling of an advanced NH_3 abatement and recycling technology in the ammonia-based CO_2 capture process. Environ Sci Technol 48(12):7179–7186
40. Li J, Henni A, Tontiwachwuthikul P (2007) Reaction kinetics of CO_2 in aqueous ethylenediamine, ethyl ethanolamine, and diethyl monoethanolamine solutions in the temperature range of 298–313 K, using the stopped-flow technique. Ind Eng Chem Res 46:4426–4434
41. Li L, Li H, Namjoshi O, Du Y, Rochelle GT (2013) Absorption rates and CO_2 solubility in new piperazine blends. Energy Procedia 37:370–385
42. Liu J, Thallapally PK, McGrail BP, Brown DR, Liu J (2012) Progress in adsorption-based CO_2 capture by metal–organic frameworks. Chem Soc Rev 41:2308–2322
43. Liu Y, Wang Z, Zhou H (2012) Recent advances in carbon dioxide capture with metal-organic frameworks. Greenhouse Gas Sci Technol 2:239–259
44. Ma'mun S, Dindore VY, Svendsen HF (2007) Kinetics of the reaction of carbon dioxide with aqueous solutions of 2-((2-aminoethyl)amino)ethanol. Ind Eng Chem Res 46:385–394
45. Mattisson T, Lyngfelt A, Leion H (2009) Chemical-looping oxygen uncoupling for combustion of solid fuels. Int J Greenhouse Gas Control 3:11–19
46. Nakayama S, Noguchi Y, Kiga T, Miyamae S, Maeda U, Kawai M, Tanaka T, Koyata K, Makino H (1992) Pulverized coal combustion in O_2/CO_2 mixtures on a power plant for CO_2 recovery. Energy Convers Manage 33(5–8):379–386
47. Oke TR (1987) Boundary layer climates, 2nd edn. Methuen, London, p 14
48. Pirngruber GD, Leinekugel-le-Cocq D (2013) Design of a pressure swing adsorption process for postcombustion CO_2 capture. Ind Eng Chem Res 52:5985–5996
49. Ramdin M, de Loos TW, Vlugt TJH (2012) State-of-the-art of CO_2 capture with ionic liquids. Ind Eng Chem Res 51:8149–8177
50. Ryden M, Lyngfelt A, Mattisson T (2011) $CaMn_{0.875}Ti_{0.125}O_3$ as oxygen carrier for chemical-looping combustion with oxygen uncoupling (CLOU)—experiments in a continuously operating fluidized-bed reactor system. Int J Greenhouse Gas Control 5:356–366

51. Seevam P, Race JM, Downie MJ, Hopkins P (2008) Transporting the next generation of CO_2 for carbon capture and storage: the impact of impurities on supercritical CO_2 pipelines. In: 2008 7th international pipeline conference, Calgary, Alberta, Canada, vol 1, pp 39–51. Paper No. IPC2008-64063, 29 Sept–3 Oct 2008
52. Smith JB, Tirpak DA (1990) The potential effects of global climate change on the United States. Hemisphere, New York
53. Torp TA, Gale J (2004) Demonstrating storage of CO_2 in geological reservoirs: the Sleipner and SACS projects. Energy 29:1361–1369
54. Vaidya PD, Kenig EY (2007) CO_2-alkanolamine reaction kinetics: a review of recent studies. Chem Eng Tech 30(11):1467–1474
55. Vega LF, Vilaseca O, Llovell F, Andreu JS (2010) Modeling ionic liquids and the solubility of gases in them: recent advances and perspectives. Fluid Phase Equilib 294:15–30
56. Xu S, Wang Y, Otto FD, Mather AE (1996) Kinetics of the reaction of carbon dioxide with 2-amino-2-methyl-1-propanol solutions. Chem Eng Sci 51(6):841–850
57. Yoon SJ, Lee H (2002) Kinetics of absorption of carbon dioxide into aqueous 2-amino-2-ethyl-1,3-propanediol solutions. Ind Eng Chem Res 41:3651–3656